SHORT TERM CONTRACT FOR THE BIOLOGICAL AND GENETIC SAMPLING AND ANALYSIS (ICCAT-GBYP 02/2013) WITHIN THE GBYP (Phase 4)

Final Report

for:

ICCAT

Scientific coordinator:

Dr. Haritz Arrizabalaga (AZTI-Tecnalia)

Pasaia, September 12th, 2014

PARTNERS:

Fundación AZTI-AZTI Fundazioa

Instituto Español de Oceanografía

IFREMER

Universitá di Genova

University of Bologna

COMBIOMA

Euskal Herriko Unibertsitatea / Universidad del País Vasco

National Research Institute of Far Seas Fisheries

INRH

Federation of Maltese Aquaculture Producers

Texas A&M University

IZOR

GMIT

SUBCONTRACTORS:

BIOGENOMICS

Laboratoire Halieutique (Algerie)

Dr. Isik Oray

CEPRR

INAPESCA

Dr. Massimiliano Valastro

INDEX:

EXECUTIVE SUMMARY:

The main objective of this project is to enhance knowledge about Atlantic bluefin tuna population structure and mixing, but also focusses on age and reproductive dynamics. The sampling protocols and structure of the data bank were revised and agreed with ICCAT Secretariat in previous Phases.

During Phase 4, the consortium has sampled a total of 2036 bluefin tuna (184 larvae, 403 YOY, 377 juveniles, 272 medium size fish, and 800 large fish) from different regions (86 from the East Mediterranean, 522 from the Central Mediterranean, 305 from the Western Mediterranean, 576 from the Northeast Atlantic, 414 from the Central North Atlantic and 133 from the Western Atlantic). From these individuals, 4176 biological samples were taken (1976 genetic samples, 1141 otoliths and 1059 spines).

Regarding otolith microchemistry, a total of 655 analyses were conducted. Carbon and oxygen isotope analyses were carried out in 327 otoliths of Atlantic bluefin tuna captured within the mixing area (central Atlantic Ocean, Morocco and Canary Islands) to determine their nursery area. $\delta^{13}C$ and $\delta^{18}O$ values measured in otolith cores indicated that the Atlantic Ocean east of 45ºW is dominated by the eastern population, whereas west of 45ºW, the majority of individuals belong to the western population. Interannual variability in the spread of western individuals towards the east was detected.

$\delta^{13}C$ and $\delta^{18}O$ values were also measured in a series of transects milled across the otolith ventral arm of 10 bluefin tuna (N=114) captured in the Bay of Biscay and Strait of Gibraltar to try to detect if these individuals have visited the western Atlantic Ocean during their lifetime. Preliminary results indicate that about half of the analyzed individuals inhabited in the western or northern Atlantic Ocean during their adolescence. However, the interpretation of these results should be made with caution, as the isotopic values obtained during the juvenile, adolescent and adult stages were directly compared to baseline dataset constructed by yearling

individuals. Although the methodology could be valid for studying transatlantic migrations, there is a need to investigate the effects of ontogeny in $\delta^{13}C$ and $\delta^{18}O$ values. The broad temporal resolution of the methodology is also a limitation, since a transect is often reflecting an integrated signal over 1 year period.

Trace element analyses by LA-ICPMS at the edge of the otoliths (N=154) indicated that Mediterranean Sea and Atlantic Ocean water masses could be discriminated based on Mg:Ca, Sr:Ca and Ba:Ca ratios. Although differences within the Mediterranean Sea were visible, an overall classification success of 78% was achieved with the concentration of these three elements. Given the high temporal resolution and the capacity to measure very low element concentrations, the methodology appears to be a promising tool to study movements of Atlantic bluefin tuna between the Atlantic Ocean and Mediterranean Sea.

Elemental analyses using LA-ICPMS were also carried out in the core of YOY bluefin tuna otoliths collected in the eastern, central and western Mediterranean Sea (N=60) to examine if the three main nursery areas could be discriminated by trace element concentration. Results indicated a high discrimination accuracy (between 73% and 85%), highlighting the potential the technique to study population structure within the Mediterranean Sea.

Regarding genetic analyses, two new research pipelines have been developed in order to overcome the overseen setbacks of the original Genotyping by Sequencing (GBS) approach. Using an improved reference genome and the GBS data generated during GBYP Phase 3, the consortium has combined the data from all individuals within 5 spawning areas and reanalyzed the data using a "Pooled data /Allele frequency approach". A panel of 384 candidate single nucleotide polymorphisms (SNPs) with potential for discriminating between populations has been developed for downstream applications and is currently being manufactured. All the samples for panel validation (192) and genotyping (576) are already selected. On the other hand, an entirely different Next Generation Sequencing (NGS) platform (Site Associated DNA sequencing or RAD-seq) was applied to 165 reference samples (larvae and young-of-the-year) from 4 spawning areas. Preliminary results show clear

differentiation of the Gulf of Mexico samples from the Mediterranean samples. This difference is more pronounced in the case of the larvae analyzed. Moreover a slight separation can be observed within the Mediterranean sea, with the Western Mediterranean larvae being different from the rest of the samples.

Regarding otolith shape analyses, 718 individuals from different age classes (juvenile, medium, large), years (2011, 2012 and 2013) and areas throughout the Atlantic and Mediterranean were analyzed. Results suggest that there exists slight but significant spatial variation in otolith shape of bluefin tuna in the East Atlantic and Mediterranean (in feeding aggregations) which is independent of variation in size and is temporally consistent. The results indicate the existence of two groups that mix to varying degrees in the different regions during feeding. In adult bluefin otolith shape varies over broad spatial scales. Fish from the west Atlantic are the most distinct.

There is a large degree of overlap in otolith shape between regions and fish can not be assigned to site of capture with acceptable levels of accuracy using otolith shape alone, but may be useful for resolving underlying structure in Atlantic bluefin tuna, when combined with information from other methods (e.g. genetics, otolith chemistry) and ideally when applied to samples of known stock origin.

Regarding the results of the age calibration exercise, a good participation with 21 readers from 13 laboratories contributed interpreting images of paired calcified structures, otoliths and spines, coming from the same specimen. The mean coefficient of variation and average per cent error were around 20 and 15 respectively. Precision was lower for inexperienced readers than for experienced ones, being experience a major factor in the age interpretation from otoliths viewed under reflected light and for large specimens using spines under transmitted light. There was generally good agreement in the ageing among different structures coming from the same specimen. Otoliths aged using different types of light showed a good agreement with no significant bias ($p>0.05$), while spine showed no sign of bias with respect to otoliths viewed under transmitted light ($p>0.05$) but a slight under ageing when compared with reflected light otoliths ($p<0.05$), with these

differences been found in specimens older than 14 years, for which the number of samples was very small. Further standardization of age reading criteria between laboratories and a description of the annual formation of otolith edge type is needed.

In general, Phase4 was importantly affected by the delay in the contract signature. However, most of the objectives of the Project were met and some were surpassed. These analyses already started to provide some results that can be refined and further explored in subsequent Phases of GBYP to provide important information relevant for Atlantic Bluefin Tuna management.

1. CONTEXT

On March 25th 2013, the consortium formed by Fundación AZTI-AZTI Fundazioa, Instituto Español de Oceanografía, IFREMER, Universitá di Genova, University of Bologna, IZOR, COMBIOMA, Euskal Herriko Unibertsitatea / Universidad del País Vasco, National Research Institute of Far Seas Fisheries, Federation of Maltese Aquaculture Producers, INRH, GMIT and Texas A&M University, with subcontracted parties Biogenomics, CEPRR, Laboratoire Halieutique Algerie, INAPESCA, CNR-IAMC, Drs. Isik Oray, and Dr. Massimiliano Valastro, coordinated by Fundación AZTI-AZTI Fundazioa, presented a proposal to the call for tenders on biological and genetic sampling and analysis (ICCAT-GBYP 02/2013).

This proposal was awarded by the Secretariat on October 7 2013. The final contract between ICCAT and the consortium represented by Fundación AZTI-AZTI Fundazioa was signed on October 18th 2013 and amended the 12th of November 2013 and again in March 31st 2014.

According to the terms of the contract, an updated preliminary report (Deliverable nº 3) was submitted to ICCAT by April 30th 2014, updating previous reports (Deliverable nº 2) with preliminary data and information useful for the Bluefin data preparatory meeting. The draft final report (Deliverable nº 4) including a detailed description of the work carried out was submitted by September 5th. The final report (Deliverable nº 5) incorporating the comments and suggestions on the draft

final report was required to be submitted by 12th of September. The present report was prepared in response to such requirement.

2. SAMPLING

The sampling conducted under this project follows a specific design, aimed primarily at contributing to knowledge on population structure and mixing. As such, the sampling conducted under this project is independent from other routine sampling activities for fisheries and fishery resources monitoring (e.g. the Data Collection Framework). Some of the sampling activities included in this report were conducted under other GBYP contracts (i.e. as part of the tagging programs).

2.1. Sampling accomplished

A total of 2036 bluefin tuna individuals have been sampled so far. Table 2.1 shows the number of bluefin tuna sampled in each strata (area/size class combination), and Table 2.2. and Figure 2.1 provide summaries by main region and size class.

The original plan, according to the extended contract, was to sample 1210 individuals (including those to be provided by the tagging cruises), thus the current sampling status represents 168% of the target in terms of number of individuals. By size class, the objectives for larvae, age 0, juveniles, medium and large fish were all accomplished (368%, 134%, 343%, 160%, 138% and 168% respectively).

Table 2.1. Number of bluefin tuna sampled by area/fishery and size class. Empty cells indicate that no sampling was planned in that stratum. Green cells indicate strata were no sampling was planned but some sampling was finally accomplished.

		Larvae	Age 0	Juveniles	Medium	Large	Total		
			<=3 kg	>3 & <=25 kg	>25 & <=100 kg	>100 kg		Target	%
Eastern Mediterranean	Levantine Sea		86				86	50	172%
Central Mediterranean	Adriatic Sea			60			60	60	100%
	Malta		50				50	50	100%
	South of Sicily and Ionian Sea	58	50	50			158	100	158%
	Gulf of Syrte				114	140	254	150	169%
Western Mediterranean	Balearic	42	134				176	110	160%
	Ligurian Sea		33				33	50	66%
	Sardinia				36	5	41	60	68%
	Algeria					0	0	50	0%
	Tyrrhenian		50		3	2	55	50	110%
Northeast Atlantic	Bay of Biscay			265	26	1	292	110	265%
	Canary Islands					89	89	50	178%
	Gibraltar			2	59		61	60	102%
	Morocco					110	110	110	100%
	Mauritania					23	23	0	>100%
	Norway					1	1	0	>100%
Central North Atlantic	Azores-Madeira					0	0	50	0%
	Central North Atlantic				34	380	414	50	828%
Northwest Atlantic	Gulf of Mexico	84				0	84	50	168%
	Gulf of Saint Lawrance					23	23	0	>100%
	Newfoundland-Labrador					9	9	0	>100%
	Nova Scotia					17	17	0	>100%
	Total	184	403	377	272	800	**2036**	1210	168%

Table 2.2: Number of bluefin tuna sampled *by main region and size class. Empty cells indicate that no sampling was planned in that strata.*

	Larvae	Age 0	Juvenile	Medium	Large	TOTAL	Target	%wrt target
East Med		86				86	50	172%
Central Med	58	100	110	114	140	522	360	145%
West Med	42	217		39	7	305	320	95%
NE Atl			267	85	224	576	330	175%
Central N Atl				34	380	414	100	414%
West Atl	84				49	133	50	266%
TOTAL	184	403	377	272	800	**2036**	1210	168%
Target	50	300	110	170	580	1210		
% wrt target	368%	134%	343%	160%	138%	168%		

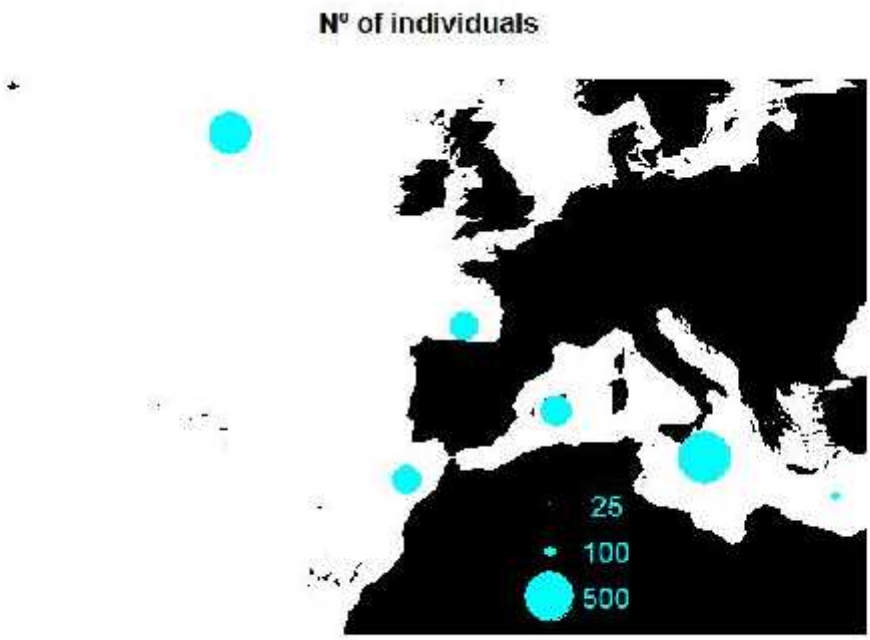

Figure 2.1: Number of individuals sampled in the Northeast Atlantic and Mediterranean, aggregated by main region. Positions of the dots are approximate averages across all samples. In the case of the North East Atlantic region, two dots are presented, one in the Atlantic side of the Strait of Gibraltar and the other in the Bay of Biscay.

The overall progress of the project was affected by the late award and signature of the contract. This affected mainly in those cases where travel, purchase and/or subcontracting costs were needed to accomplish the tasks. Yet, the sampling objectives were met.

In the Eastern Mediterranean, 172% of the target number of individuals (YOY) has been sampled. In the Central Mediterranean, 145% of the target number of individuals has been sampled, including fish of all size classes (larvae, YOY, juvenile, medium and large fish). Larvae previously expected to be delivered to UNIBO from a sub-contracted party and collected from the Southern Ionian Sea in 2013 were unfortunately unavailable due to unforeseen logistical re-arrangements. UNIBO have in turn arranged for the use of larvae from the same approximate geographical location from IEO, collected during a larvae survey conducted in 2008. This change was reflected in the amended contract.

These samples will provide not only important spatial data but also essential temporal genetic information.

In the Western Mediterranean, 95% of the target number of individuals was sampled, including mainly reference samples (larvae and YOY) as well as medium size fish. The provision of samples from large fish by the tagging surveys did not result as expected, and the genetic sampling of large fish in Algeria could neither be materialized by the consortium. However, this was compensated by sampling of other size classes (e.g. medium fish in Sardinia). IEO also provided a 2012 larval sample from the Balearics that was helpful for the genetic analyses.

In the North East Atlantic, 175% of the target number of individuals was sampled, including juvenile, medium and large fish. Sampling of large and medium fish in the Bay of Biscay was below expectations, which was compensated by juvenile fish. The samples of Morocco and the Canary Islands provide opportunities to further inspect mixing in this area. Furthermore, although small quantities, unexpected samples from Norway (IMR) and Mauritania (CROD) were obtained.

In the Central North Atlantic, 414% of the target number of individuals was sampled, mostly large but also some medium fish, which was not originally planned. Efforts to sample in the Azores were not fruitful, but this was compensated by Central Atlantic samples provided by Japanese scientists belonging mostly to the 2012 fishing season.

Finally in the Western Atlantic, 266% of the target number of individuals was sampled. Although the Consortium could not get samples from large fish in the Gulf of Mexico, this was compensated by large fish samples provided by Canadian colleagues (DFO). Moreover, additional larval tissue was provided by US colleagues (TAMU and USC) as needed for genetic analyses.

Tables 2.3. and 2.4 as well as Figures 2.2, 2.3 and 2.4 show the number of different tissues sampled in each area. Because not all biological samples have been received at AZTI yet, and thus verified, the list of biological samples available might have some slight changes in the future. According to it, 4176 biological samples have been collected so far in Phase 4. In many cases, not all tissues (otoliths, muscle or fin for genetics, and/or spine, according to the sampling scheme) were collected from each single fish.

However, both the total amount of samples as well as the number of samples by tissue type (1141 otoliths, 1059 spines and 1976 genetic samples) is high and relatively well distributed over the different main regions (considering the late signature of the contract and the circumstances explained in earlier paragraphs).

Table 2.3: Number of samples collected by area/fishery and tissue type:

		Otolith	Spine	Muscle/Fin	Sampler
Eastern Mediterranean	Levantine Sea	85	85	86	AZTI (Oray)
Central Mediterranean	Adriatic Sea	60	60	60	IZOR
	Malta	50	50	50	FMAP
	South of Sicily and Ionian Sea	100	100	158	UNIBO/IEO
	Gulf of Syrta		254	254	FMAP
Western Mediterranean	Balearic	103	103	176	AZTI/IEO
	Ligurian	33	33	33	UNIGE
	Sardinia		41	40	UNICA
	Tyrrhenian	54	54	54	UNIBO
Northeast Atlantic	Bay of Biscay	138	192	281	AZTI
	Canary Islands	64		49	IEO
	Gibraltar	61	61	61	IEO
	Morocco	110	26	110	INRH
	Mauritania			23	AZTI (CROD)
	Norway			1	AZTI(IMR)
Central North Atlantic	Central North Atlantic	283		407	NRIFSF
Western Atlantic	Gulf of Mexico			84	TAMU/AZTI(USC)
	Gulf of Saint Lawrance			23	AZTI(DFO)
	Newfoundland-Labrador			9	AZTI(DFO)
	Nova Scotia			17	AZTI(DFO)
TOTAL		**1141**	**1059**	**1976**	
			4176		

Table 2.4: Number of samples by main region and tissue type:

	Otolith	Spine	Muscle/Fin	TOTAL
East Med	85	85	86	256
Central Med	210	464	522	1196
West Med	190	231	303	724
NE Atl	373	279	525	1177
Central N Atl	283		407	690
West Atl			133	133
TOTAL	**1141**	**1059**	**1976**	**4176**
Target	910	1110	1160	3180
% wrt target	125%	95%	170%	131%

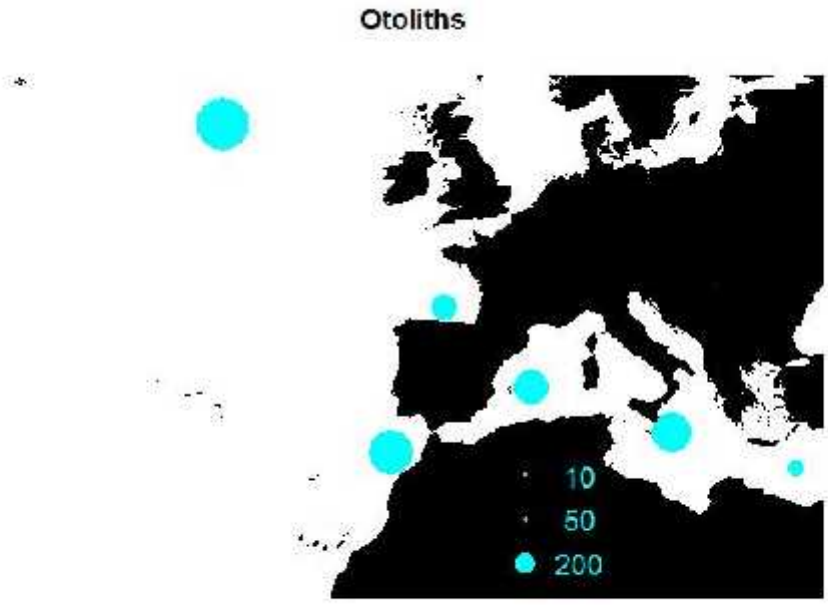

Figure 2.2: Number of individuals with otolith sampling in the Northeast Atlantic and Mediterranean, aggregated by main region. Positions of the dots are approximate averages across all samples. In the case of the North East Atlantic region, two dots are presented, one in the Atlantic side of the Strait of Gibraltar and the other in the Bay of Biscay.

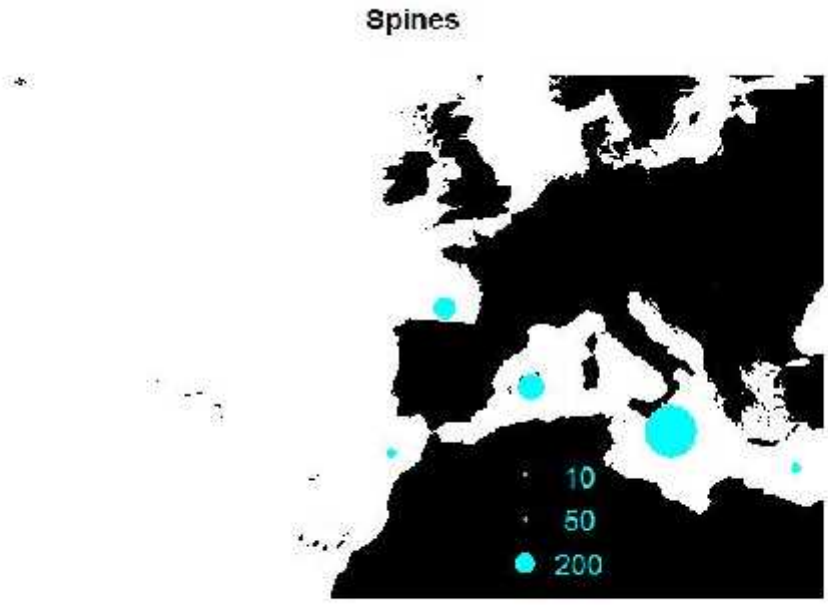

Figure 2.3: Number of spines collected in the Northeast Atlantic and Mediterranean, aggregated by main region. Positions of the dots are approximate averages across all samples. In the case of the North East Atlantic region, two dots are presented, one in the Atlantic side of the Strait of Gibraltar and the other in the Bay of Biscay.

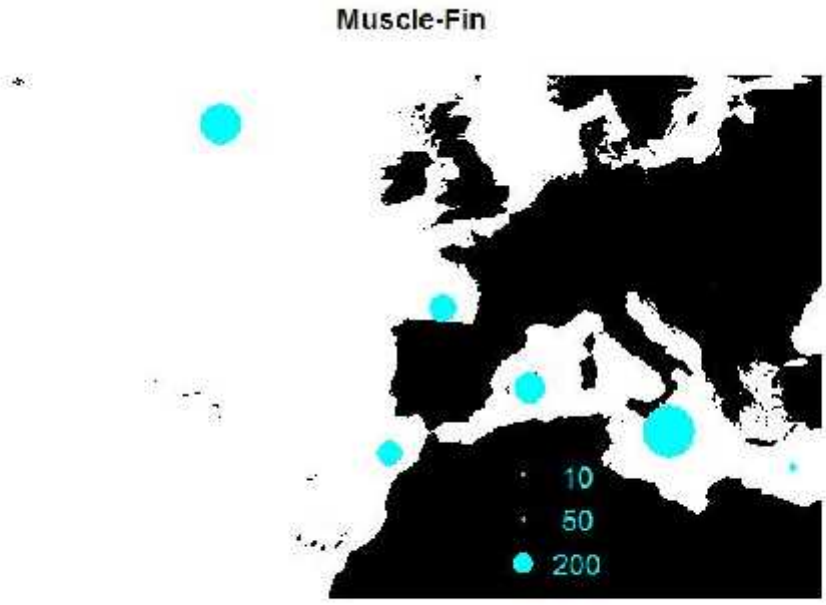

Figure 2.4: Number of muscle or fin tissue samples collected in the Northeast Atlantic and Mediterranean, aggregated by main region. Positions of the dots are approximate averages across all samples. In the case of the North East Atlantic region, two dots are presented, one in the Atlantic side of the Strait of Gibraltar and the other in the Bay of Biscay.

Most of these samples have been sent to AZTI, following the protocols (although some samples were directly sent to the analyst due to time constraints). This step allows for quality control of the samples and the coding, as well as fulfilling the requirement of having a centralized collection of samples for future use. The samples are conserved following the protocols and stored in the central facilities of AZTI-Tecnalia in Pasaia (contact persons: Igaratza Fraile and Nicolas Goñi). The samples already distributed to other labs (for analyses under different tasks) are tagged in the database.

3. ANALYSES

In the proposal, the consortium proposed to analyze a subset of 500 otoliths (for microchemistry), 888 muscle/fin samples for genetic analyses (120 with Rad-Seq and 768 with GBS), 300 otolith images for otolith shape analysis, and three sets of 100 images (otoliths with transmitted and reflected light, and spines under transmitted light) for the age calibration analysis,. As reflected in the Interim Report, the late start of the contract affected the ability of partners to conduct sampling, send samples to AZTI, proceed with planned subcontracts, etc. implying that availability of checked samples for analyses was generally low. On top of this, the tight deadlines for conducting the analyses and the time needed to accomplish them urged to start analyses as soon as possible. This, in some cases, limited the samples that were analyzed to those that were available at the time of starting the analyses.

The following sections reflect the status of analyses conducted by the consortium. The samples that were not analyzed yet remain stored in AZTI for future analyses, where a more optimized design of the different analyses can be approached.

4. OTOLITH MICROCHEMICAL ANALYSES

Task Leader: Jay Rooker (TAMUG)

Participants:

AZTI: Igaratza Fraile, Haritz Arrizabalaga

TAMU: Jay Rooker

NRC: Anna Traina

4.1. General overview

Several novel tools are currently being used to investigate the natal origin and stock structure of Atlantic bluefin tuna, including electronic tags, molecular genetics, and otolith chemistry. Of the three, chemical markers in otoliths (ear stones) have significant potential for determining natal origin and population connectivity of bluefin tuna (Rooker et al. 2007). This is due to the fact that otoliths precipitate material (primarily calcium carbonate) as a fish grows, and the chemical composition of each newly accreted layer is often associated with physicochemical conditions of the water mass they inhabit. As a result, material deposited in the otolith during the first year of life serves as a natural marker of the individual's nursery or place of origin. Previous studies have demonstrated that trace elements and stable isotopes in otoliths can be used to determine the origin of bluefin tuna from different regions in the Atlantic Ocean and its marginal seas (Mediterranean Sea and Gulf of Mexico; see Rooker et al. 2008a,b, Schloesser et al. 2010). Results from these studies indicate that trans-Atlantic movement is more significant than previously assumed, with a considerable fraction of adolescents in US water originating from spawning/nursery areas in the east (Mediterranean Sea).

4.2. Origin of Atlantic bluefin tuna in the North Atlantic Ocean using $\delta^{13}C$ and $\delta^{18}O$ in otoliths

In this section, we investigate the origin of bluefin tuna collected in the central North Atlantic Ocean (east and west of 45ºW) and eastern North Atlantic Ocean (Moroccan coast and Canary Islands) using stable $\delta^{13}C$ and $\delta^{18}O$ isotopes in otoliths. Samples utilized for this study were collected under the GBYP. Central Atlantic (east of 45ºW) samples were collected in October-November of 2011 and 2012 by observers on board of Japanese longline fleet operating south of Iceland (53-59ºN, 19-20ºW) whereas central North Atlantic (west of 45ºW) samples were captured in September 2012 (44-47ºN, 47-48ºW). Samples from eastern North Atlantic were collected in May 2012 and 2013 by Moroccan traps, off the African continent (35ºN, 6ºW approximately), and during March 2013 around Canary Islands (Fig. 4.1). Otolith handling followed the protocols previously described in Rooker et al. (2008b). Briefly, following extraction by GBYP participants, sagittal otoliths of bluefin tuna were cleaned of excess tissue with nitric acid (1%) and deionized water. One sagittal otolith from each bluefin tuna specimen was embedded in Struers epoxy resin (EpoFix) and sectioned using a low speed ISOMET saw to obtain 1.5 mm transverse sections that included the core. Following attachment to a sample plate, the portion of the otolith core corresponding to approximately the yearling periods of bluefin tuna was milled from the otolith section using a New Wave Research MicroMill system. A two-vector drill path based upon otolith measurements of several yearling bluefin tuna was created and used as the standard template to isolate core material following Rooker et al. (2008b). The pre-programmed drill path was made using a 500 μm diameter drill bit and 15 passes each at a depth of 50 μm was used to obtain core material from the otolith. Powdered core material was transferred to silver capsules and later analyzed for $\delta^{13}C$ and $\delta^{18}O$ on an automated carbonate preparation device (KIEL-III) coupled to a gas-ratio mass spectrometer (Finnigan MAT 252). Stable $\delta^{13}C$ and $\delta^{18}O$ isotopes are reported relative to the PeeDee belemnite (PDB) scale after comparison to an in-house laboratory standard calibrated to PDB.

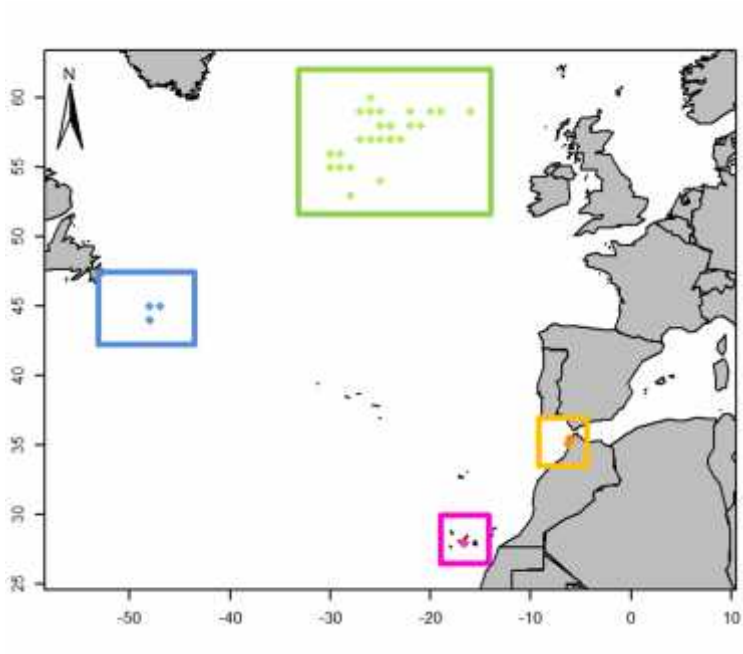

Figure 4.1: Study area in the North Atlantic Ocean. Otoliths collected in the central Atlantic (west of 45ºW, blue), central Atlantic (east of 45ºW, green), Moroccan coast (orange) and around Canary islands (pink).

Region-specific estimates of nursery origin of bluefin tuna were based on comparing otolith 'cores' (corresponds otolith material deposited during the first year of life or yearling period) of adult bluefin tuna to the baseline or reference samples of yearling bluefin tuna. Estimate of origin for adult (medium and large) bluefin tuna were obtained using the maximum likelihood estimate (MLE) from the mixed-stock program HISEA developed by Millar (1990). Baseline data for mixed-stock analysis was otolith $\delta^{13}C$ and $\delta^{18}O$ of yearling samples collected in the east and west from 2000-2012, with recent samples (e.g. 2009-2011) supplied through GBYP. Otolith cores of adult bluefin tuna collected in the central and eastern Atlantic Ocean were then used to estimate the origin of these recruits in the bootstrap mode of HISEA, which provided non-parametric estimates of the reliability of predicted contributions from eastern (Mediterranean) and western (Gulf of Mexico) spawning grounds.

$\delta^{13}C$ and $\delta^{18}O$ were measured in the otolith cores of large (>100 kg) bluefin tuna from different locations in the Atlantic Ocean between October 2011 and May 2013: 1) central North Atlantic (east of 45ºW; year=2011, n=28), 2) central North Atlantic (west of 45ºW; year=2012,n=18), 3) central North Atlantic (east of 45ºW; year=2012, n=150), 4)

Morocco (year=2012, n=49), 5) Canary Islands (year=2013, n=20) and 6) Morocco (year=2013, n=59) (for detailed information see Table 4.1).

Mixed-stock analysis based on maximum-likelihood estimates (MLE) indicated that bluefin tuna collected south of Iceland and in Moroccan waters (during October-November 2011 and May 2012 respectively) were determined to be entirely comprised by individuals from the 'eastern' or Mediterranean nursery (Fig. 4.2 and 4.3, Table 4.2). Standard deviation around estimated percentages was + 0%, indicating the degree of confidence in our predicted assignment was high. In September 2012, the majority of bluefin tuna captured by Japanese longliners in the central North Atlantic (west of 45ºW) were from the western nursery (94%), whereas catches during the next months in the central North Atlantic (east of 45ºW) were dominated by the eastern population (83%) (Fig. 4.3, Table 4.2). During 2013 isotopic analyses revealed mixing in of the two populations in the eastern North Atlantic, where a large proportion of western origin bluefin tuna were found around Canary Islands (21% of western origin vs. 79% of eastern origin) and a lower degree of mixing found in Moroccan traps (98% from eastern population). However, in the latest two locations the errors around the estimated proportions exceed the 95% confidence intervals (1.96*SD) and thus using MLE western contribution around Canary Islands and off Africa cannot be confirmed.

Previous analyses carried out in Phases 2 and 3 with samples collected in 2010 and 2011 suggested a high degree of mixing off the coast of Africa. However, the presence of western migrants in the present study was null in 2012 and limited (if any) in 2013, suggesting that west to east transatlantic movements may not have the same range every year. In the same way, notable mixing rates in the central Atlantic Ocean have been detected in previous samples, particularly in the western side of the management boundary. Our results are in agreement with previous findings, confirming that west of 45ºW bluefin tuna is largely dominated by the western population, whereas east of 45ºW in the central North Atlantic (south of Iceland) mixing of the two populations varies from year to year, but predominantly individuals from the eastern nursery are found in this area.

Interannual variations may be important in the spatial distribution of bluefin tuna in the North Atlantic Ocean. Our results suggest that during the end of 2011 and beginning of 2012, the western population may have stayed concentrated in the western

side of the Atlantic Ocean, whereas at the end of 2012 and beginning of 2013 individuals from the western nursery may had a different distribution resulting in the spread of individuals towards the east, and covering a wide range of the North Atlantic Ocean.

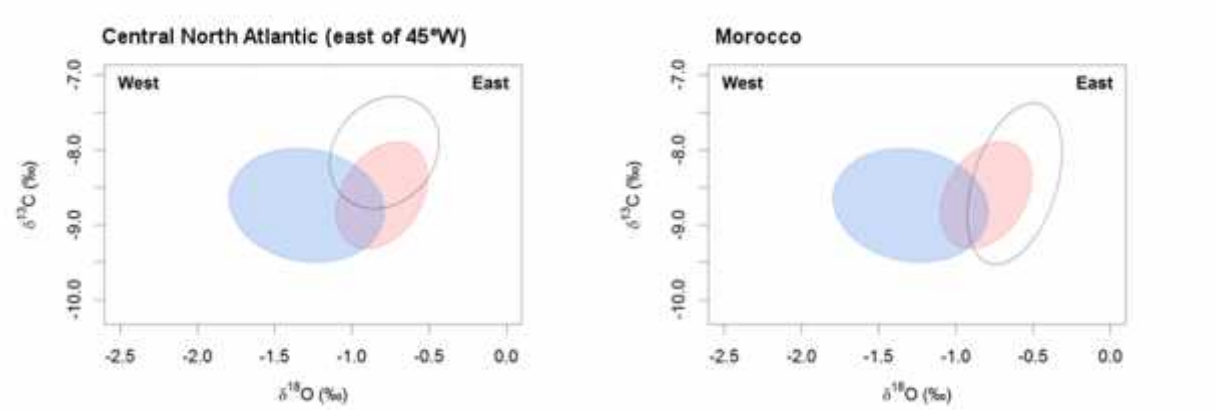

Figure 4.2: Confidence ellipses (1 SD or ca. 68% of sample) for otolith ¢^{13}C and ¢^{18}O values of yearling bluefin tuna from the east (red) and west (blue) along with the confidence ellipse (black line) for otolith cores of large bluefin tuna of unknown origin collected in the northern North Atlantic (south of Iceland) during October-November 2011 and eastern North Atlantic (off Morocco) in May 2012.

Table 4.1. *Maximum-likelihood predictions of the origin of large (>100 kg) bluefin tuna collected from central and eastern North Atlantic Ocean. Estimates are given as percentages and the mixed-stock analysis (HISEA program) was run under bootstrap mode with 1000 runs to obtain standard deviations around estimated percentages (ï %).*

			Predicted Origin		
Region	**year**	**N**	**% East**	**% West**	**% SD**
Central North Atlantic (east of 45ºW)	2011	28	100	0	± 0.0
Central North Atlantic (east of 45ºW)	2012	150	83	17	± 6.4
Central North Atlantic (west of 45ºW)	2012	18	6	94	± 7.8
Morocco	2012	49	100	0	±0.0
Morocco	2013	59	98	2	+ 4.3
Canary Islands	2013	23	79	21	+ 14.0

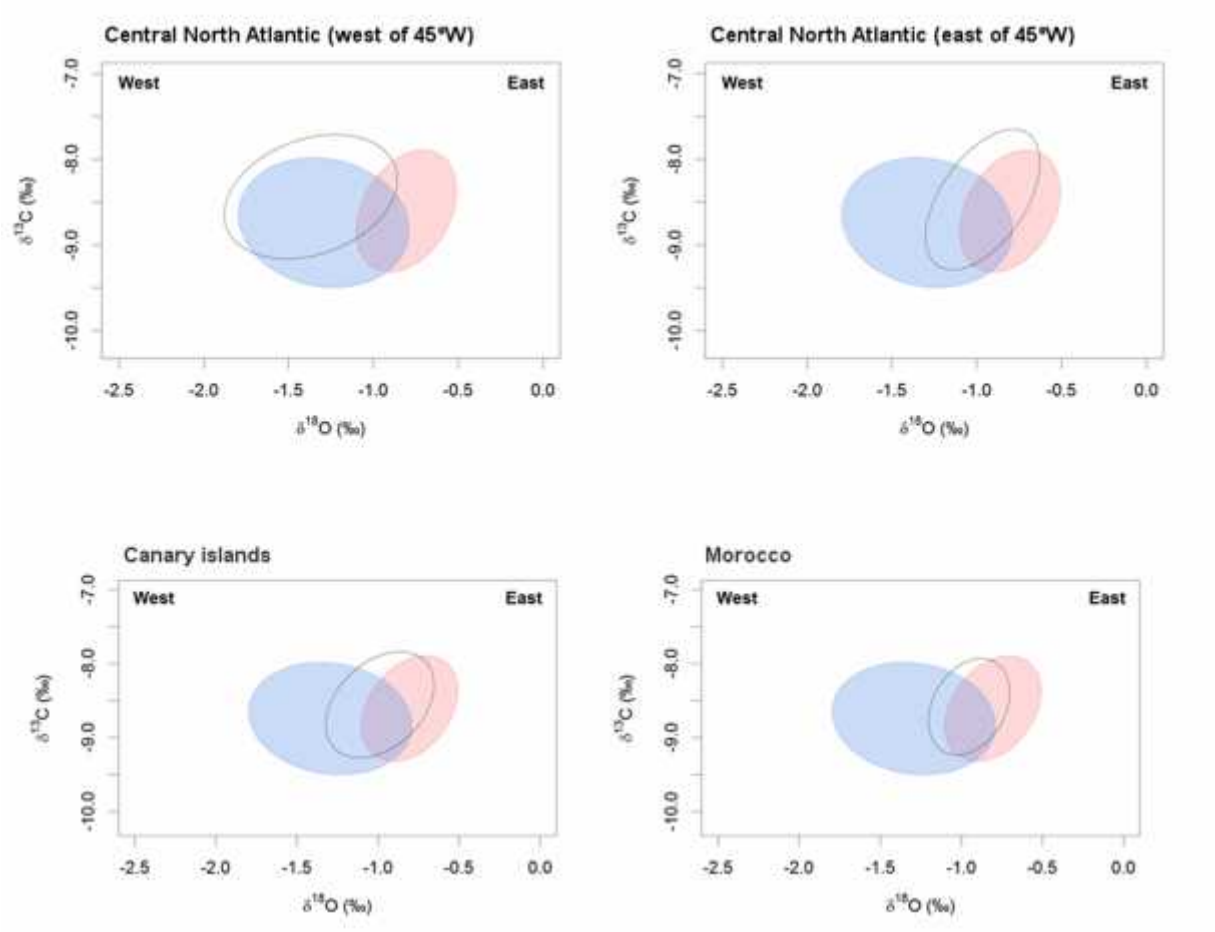

Figure 4.3. Confidence ellipses (1 SD or ca. 68% of sample) for otolith ¢^{13}C and ¢^{18}O values of yearling bluefin tuna from the east (red) and west (blue) along with the confidence ellipse (black line) for otolith cores of large bluefin tuna of unknown origin collected in the central North Atlantic (west of 45°W) during September 2012, central North Atlantic (east of 45°W) in October-November 2012, Canary islands in March 2013 and Moroccan coast in May 2013.

4.3. Discrimination of Mediterranean Sea and Atlantic Ocean water masses by otolith edge trace element composition

In order to develop new markers that allow bluefin tuna movement tracking at higher resolution, trace element analyses were carried out using Laser Ablation Inductively Coupled Plasma Mass Spectrometry (LA-ICPMS). Samples utilized for this study were collected in different regions of the eastern, central and western Mediterranean Sea, as well as open Atlantic Ocean including Bay of Biscay and Strait of Gibraltar (total n=154). Sagittal otoliths of juvenile (<25 Kg), medium (25-100 Kg) and large (>100 Kg) bluefin tuna were used. Transverse sections of approximately 0.7mm were first polished to the core with 1200 grade wet and dry sandpaper moistened with distilled water, and were further polished with a micro cloth and 0.3µm alumina powder to ensure a smooth surface. Sections were glued in a sample plate with thermoplastic glue. Magnesium (Mg), Zink (Zn), Strontium (Sr) and Barium (Ba) concentrations were measured by laser ablation inductively-coupled mass spectrometry (LA-ICP-MS) at the edge of the ventral arm of the otolith, as this portion of the otolith is supposed to reflect water mass physico-chemical properties just prior its capture. The system consisted of a laser ablation system (Nd:Yag 213 nm, New Wave Research) coupled to a mass spectrometer (X Series 2 ICP-MS, Thermo Electron Corporation). Several ablations were performed using a 40µm spot-size along the edge of the postrostrum side of the otolith, perpendicular to the growth axis (Fig. 4.4). The calibration of the ICPMS was examined using the certified reference material, NIST 612 SRM, distributed by the National Institute of Standards and Technology. Calcium concentration was assumed from the stoichiometry of calcium carbonate to be 400.000µg g-1 and the concentrations of other elements were expressed as element:Ca ratio. Multivariate statistics were then used to compare elemental composition in otoliths of bluefin tuna captured in Atlantic Ocean and Mediterranean Sea.

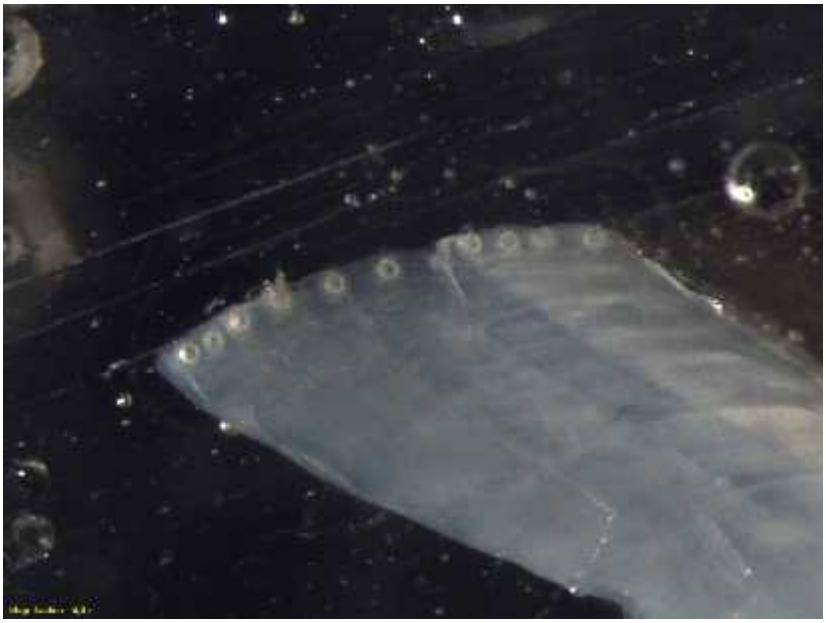

Figure 4.4: Photograph of the laser-ablation inductively coupled plasma mass spectrometry measurements along the edge of postrostrum side of the otolith.

From all the elements analysed only four were well above the detection limits: Mg, Zn, Sr and Ba. These four elements were measured in otolith edges of juvenile, medium and large bluefin tuna from several locations of the Atlantic Ocean (including Bay of Biscay (n=22), central North Atlantic Ocean (n=38) and Strait of Gibraltar (n=20)) and Mediterranean Sea (including Adriatic Sea (n=6), Ligurian Sea (n=5), Maltese waters (n=10), south of Sicily (n=6), Tyrrhenian Sea (n=10), Balearic Sea (n=6), Gulf of Lion (n=12) and Levantine Sea (n=19)) captured between 2010 and 2012 (Table 4.2). Analyses on trace elements of otolith edges showed high variability in Zn concentration within each of the otoliths. Previous works have reported that otolith Zn content is associated with the soluble part of the protein matrix, and its variations are therefore related with the fish's physiology rather than with the water chemistry (Miller et al., 2006; Sturrock et al., 2012). Zn is an essential metal for fish that plays an important role in reproduction and in immune functions (Watanabe et al., 1997). Given the complexity of its incorporation to the otolith, Zn measurements were excluded from our analysis. For the remaining elements, data from the consecutive ablation spots were averaged for each otolith.

Table 4.2. Number of otolith edges analyzed using LA-ICPMS for each of the strata

		N by Category			N
Region	**Sub-region**	**J**	**M**	**L**	**TOTAL**
Atlantic Ocean	Bay of Biscay	19	3	-	**22**
	Central North Atlantic	-	15	23	**38**
	Strait of Gibraltar	-	6	14	**20**
Mediterranean Sea	Adriatic Sea	6	-	-	**6**
	Ligurian Sea	-	5	-	**5**
	Maltese waters	-	2	8	**10**
	South Sicily	6	-	-	**6**
	Tyrrhenian Sea	-	10	-	**10**
	Balearic Sea	1	5		**6**
	Gulf of Lion	7	5	-	**12**
	Levantine Sea	-	12	7	**19**

In a first exploratory analysis, comparisons of otolith chemical composition between the bluefin tuna caught within the Mediterranean Sea and those caught in North Atlantic Ocean were made with the null hypothesis of no difference, and Mann-Whitney-Wilcoxon test was used as the test statistic. Capture location (Mediterranean Sea and Atlantic Ocean) could be discriminated based on the otolith edge signature comprising the three element ratios (Mg:Ca, Sr:Ca and Ba:Ca; Mann-Whitney-Wilcoxon test, $p<0.05$). Otolith edges showed higher Sr:Ca and Ba:Ca ratios and lower in Mg:Ca ratio for bluefin tuna captured in Mediterranean Sea compared to those captured in the Atlantic Ocean. In a second step, habitat discrimination capacity between these two groups based on otolith chemical composition was evaluated by statistical classification methods. Quadratic Discriminant Function Analysis (QDFA) was used for multivariate classification of the groups to their corresponding capture location on the basis of the

element:Ca ratios at the otolith edge. A forward stepwise classification procedure was used to select the combination of elements that optimised discrimination success of the QDFA (Mecier et al., 2011). Habitat discrimination was maximized when the combination of Mg:Ca, Sr:Ca and Ba:Ca ratios were used. Cross validated classification success (based on quadratic discriminant function analysis) of the Atlantic and Mediterranean samples was of 78% (Table 4.3).

A Principal Component Analysis (PCA) was applied to reduce the dimensionality of the data and illustrate the affinity of the elements analyzed (Fig. 4.5). The first two eigenvalues (axes) of the PCA explained >86% of the total variance. PC1 scores received positive weightings from Sr and Ba concentration, whereas PC2 score was positively associated with Mg concentration. Otoliths of bluefin tuna captured within the Mediterranean Sea were positively associated with PC1, although a high variability between different sub-regions was visible. PC2 was positively related with samples collected in different areas of the open Atlantic Ocean. Differences within the sub-regions within the Mediterranean were visible (Fig.4.5d-e-f). For example, bluefin tuna collected in the Adriatic Sea reflected a chemical signal somewhat different to the rest of the fish captured in the Mediterranean Sea, which may be due to the particular physicochemical properties of this region. Surprisingly, bluefin tuna captured southern Sicily reflect a chemical signature that seem to be closer to Atlantic samples.

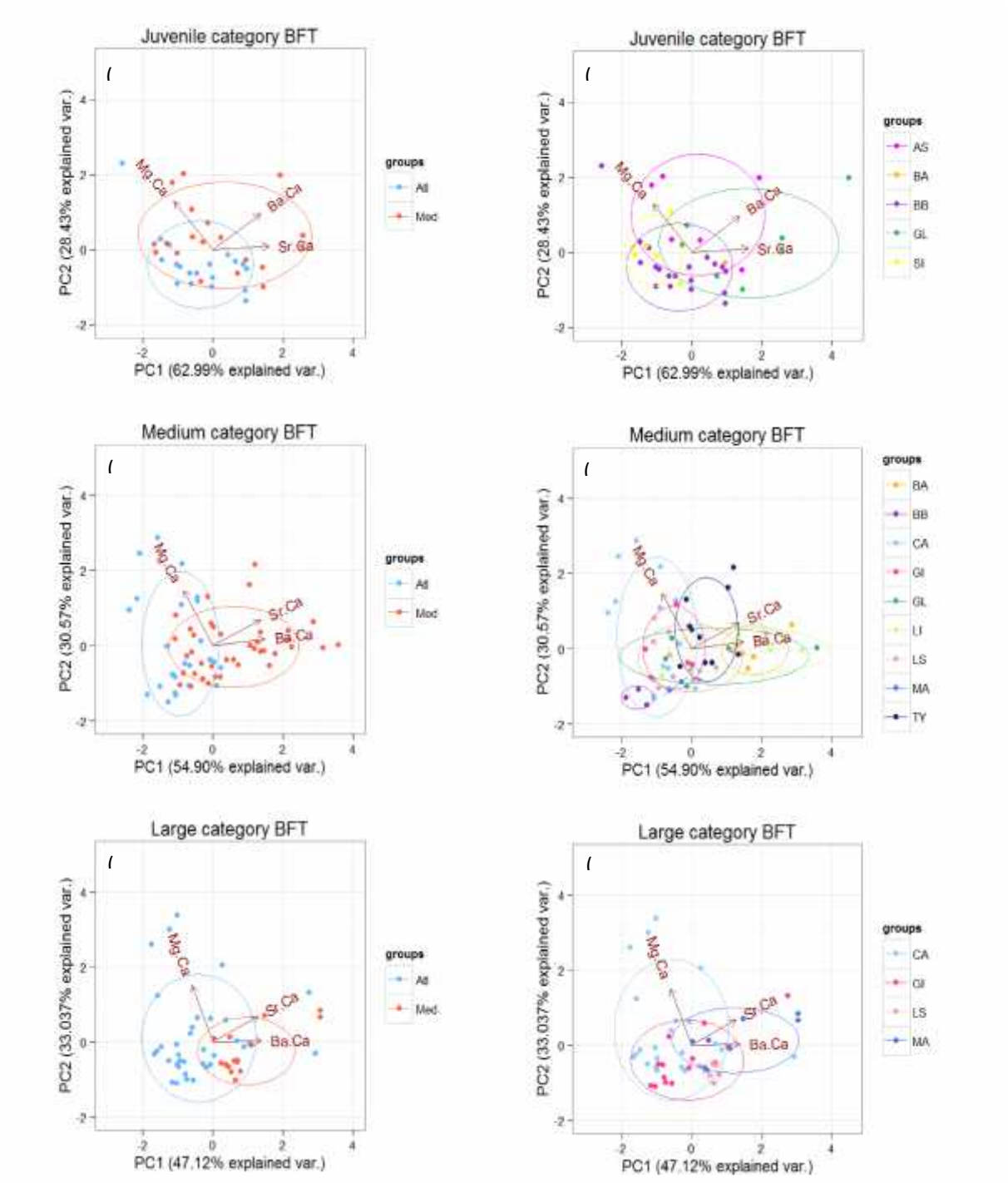

Figure 4.5 Principal Component Analysis (PCA) biplot for trace element concentration measured at the edge of bluefin tuna otoliths collected in different regions of the Atlantic Ocean and Mediterranean Sea by size categories. Arrows represent the correlation of the element:Ca ratios with the first two dimensions of the PCA (PC1 and PC2), and the points correspond to the PC1 and PC2 scores of each observation, with normal confidence ellipses (68%). (a) Biplot of elemental signatures of Atlantic Ocean (including Strait of Gibraltar) and Mediterranean Sea for juvenile category (< 25 Kg)

bluefin tuna; (b) Biplot of elemental signatures of Atlantic Ocean (including Strait of Gibraltar) and Mediterranean Sea for medium category (25-100 Kg) bluefin tuna ; (c) Biplot of elemental signatures of Atlantic Ocean (including Strait of Gibraltar) and Mediterranean Sea for large category (>100 Kg) bluefin tuna; (d)) Biplot of elemental signatures of otoliths by sub-region (Bay of Biscay (BB), Adriatic Sea (AS), Balearic Sea (BA), Gulf of Lion (GL) and South of Sicily (SI)) for juvenile category (< 25 Kg) bluefin tuna; (e) Biplot of elemental signatures of otoliths by sub-region (Bay of Biscay (BB), Central Atlantic (CA), Strait of Gibraltar (GI), Balearic Sea (BA), Gulf of Lion (GL), Ligurian Sea (LI), Levantine Sea (LS), Maltese waters (MA) and Tyrrhenian Sea (TY)) for medium category (25-100 Kg) bluefin tuna; (f) Biplot of elemental signatures of otoliths by sub-region (Central Atlantic (CA), Strait of Gibraltar (GI), Levantine Sea (LS) and Maltese waters (MA)) for large category (>100 Kg) bluefin tuna.

When analyzing these data by size categories, it is remarkable that the Atlantic and Mediterranean signatures overlap considerably in juvenile category bluefin tuna (< 25Kg), whereas medium and large size tuna show a more distinct signal (Fig. 4.5a,b and c). For juvenile bluefin tuna, only Ba concentration between the Atlantic and Mediterranean samples differ significantly (Mann-Whitney-Wilcoxon test, $p<0.05$), but Sr and Mg do not. Discrimination of juvenile bluefin tuna among the Mediterranean Sea and Atlantic Ocean using elemental concentration at the edge of the otolith was relatively high with a cross validated classification success of 82% (based on quadratic discriminant function analysis). Discrimination was driven by Ba:Ca concentration. For larger bluefin tuna, capture locations were best discriminated based on the combination of Ba:Ca, Mg:Ca and Sr:Ca concentrations. For medium size category, classification success was of 81%, followed by the large size category (73%). Overall, when all size classes were pulled together, 78% of fish were correctly classified using otolith edge signature comprised by the three element ratios (Ba:Ca, Mg:Ca and Sr:Ca) (Table 3).

The relative overlap seen in the juvenile category tuna is mostly driven by 1 year old bluefin tuna captured south of Sicily and, to a lesser extent, by 3 year old bluefin tuna from the Adriatic Sea (Fig. 4.5d). These two groups show a chemical signature that is closer from Atlantic samples than the rest of the Mediterranean otoliths. However, it is still difficult to determine if this difference is caused by the physic-chemical properties of these regions, or the fish captured in these regions could have entered the

Mediterranean Sea not long ago and thus, they still preserve the chemical signature of the open Atlantic Ocean. Samples grouped into the "central Atlantic (CA) subregion have been collected in a wide geographic area, and that is reflected in the wide range of element concentration variability shown in Fig.4.5e and 7f, particularly in the y-axis, which is predominantly dominated by the Mg:Ca concentration. In a similar way, otoliths from the Ligurian Sea (LI) and Gulf of Lion (GL) present high variability in x-axis, which summarizes the effect of Ba:Ca and Sr:Ca ratio. In these cases, the variability could be more related to changes in water mass properties due to river runoff for example, or bluefin tuna captured here could have rather moved just prior their capture. In contrast, samples collected in Balearic Sea (BA) or Levantine Sea (LS, especially large category bluefin tuna) present a contracted confidence ellipse, reflecting the similarity in the otolith signature between individual fish and thus, stability of water properties and limited movement of fish.

Table 4.3: Classification accuracy of bluefin tuna caught in the Atlantic Ocean and Mediterranean Sea based on otolith elemental concentration at the edge of the ventral arm. Classification accuracy was estimated by cross validation using quadratic discriminant function analysis (QDFA). The combination of elements that optimized classification accuracy was estimated using a forward stepwise classification procedure.

	Classification accuracy (%)	Combination of elements
Juvenile	82%	Ba:Ca
Medium	81%	Ba:Ca, Mg:Ca and Sr:Ca
Large	73%	Ba:Ca, Mg:Ca and Sr:Ca
All categories together	78%	Ba:Ca, Mg:Ca and Sr:Ca

Although region specific differences exist within the Mediterranean sea and also in the different areas of the Atlantic Ocean, the overall signature between these two big water masses can be distinguished with a relatively high accuracy (between 73% and 82% depending on the size classes). Overall, Mediterranean samples are characterized by higher Ba and Sr concentrations compared to open Atlantic Ocean samples. The new marker based on Ba:Ca, Mg:Ca and Sr:Ca ratios developed during this project could

potentially be used to detect movements into and out of the Mediterranean Sea, by applying trace element analysis along the otolith growth axis.

4.4. Discrimination of nursery areas within the Mediterranean Sea by elemental composition in otoliths of young-of-the-year bluefin tuna

Given that the material deposited during the early life period provides information about physicochemical conditions of the nursery area or place of origin of fish, we assessed the utility of otolith trace element composition in young-of-the-year (YOY, age-0) bluefin tuna to distinguish different nurseries within the Mediterranean Sea. Trace element analyses were carried out using Laser Ablation Inductively Coupled Plasma Mass Spectrometry (LA-ICPMS). Sixty samples of YOY bluefin tuna were collected from July until September 2012 from different putative nursery areas in western (Balearic Sea), central (Tyrrhenian Sea), and eastern (Levantine Sea) Mediterranean Sea (Fig. 4.6). Sagittal otoliths of YOY fish (200-460mm FL) were handled following the above described protocol. Each otolith was embedded in Struers epoxy resin (EpoFix) and sectioned using a low speed diamond-blade ISOMET saw to obtain 1.5 mm transverse sections that included the core (Rooker et al., 2014). Sections were rinsed with deionized water (DIH2O for trace metals) prior to being examined, mounted (5 per slide) whit glue (Crystalbond™ 590) on glass slide. Otolith thin sections were polished to the core using wet-dry sandpaper and 3 um aluminum oxide, and then rinsed with Milli-Q water. Polished sections were triple rinsed and air dried under a laminar flow hood. Trace element chemistry of polished otoliths was determined using a laser ablation inductively coupled plasma mass spectrometer, LA-ICP-MS (XSeries 2, Thermo Scientific ICP-MS and New Wave Research NWR 213 laser system) at Texas A&M University at Galveston. The calibration of the instrument was achieved using certified reference material (NIST 614) distributed by the National Institute of Standards and Technology. Standard was analyzed before and after each otolith, 44Ca was used as internal standard and its concentration normalized to be 380,000 μg/g. The "core signature" of Litium (Li), Magnesium (Mg), Manganese (Mn), Cobalt (Co), Cupper (Cu), Zink (Zn) Strontium (Sr) and Barium (Ba) was evaluated with a suite of 6 spots laser ablation (diameter of 50μm) carried out across the otolith surface: (n=6) extending out ~150 μm from the focus (i.e., central point) on dorsal ridge. The concentrations of other elements were expressed as element:Ca ratio

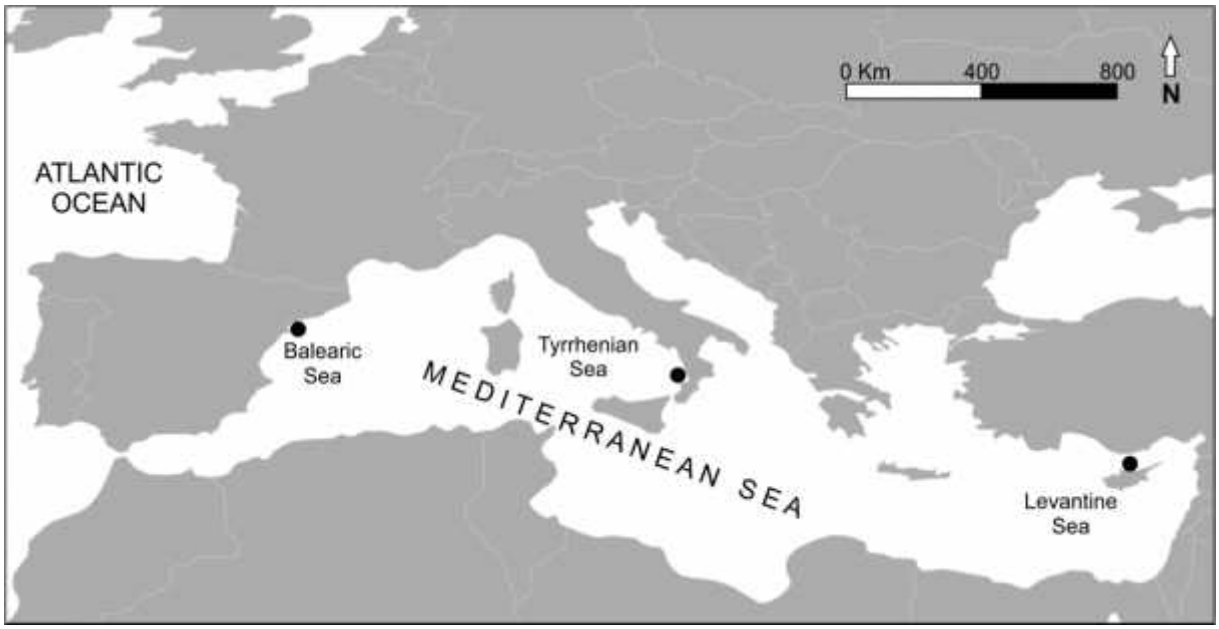

Figure 4.6: Study area in the eastern central and western Mediterranean Sea

Multivariate analysis of variance (MANOVA) was performed on all elemen:Ca ratio to verify differences among the three groups. Also quadratic discriminant function analysis (QDFA) was performed and the resultant discriminant functions were used to classify otoliths into groups and then to compare them with the origin areas. The expected error rates of the classification functions were estimated using cross-validation by the leaving-one-out procedure (Fung, 1996). A further Random Forest analysis (RF) (Breiman, 2001) was used in order to estimate the importance of trace elements concentrations to discriminate the different areas (Liaw and Wiener, 2002).

Otoliths of YOY bluefin tuna from the eastern (N=20), central (N=20) and western (n=20) Mediterranean Sea were selected for nursery discrimination within the Mediterranean Sea by elemental composition (Table 4.4). Multivariate analysis of variance shows that chemical core signature differ among the three nursery areas (MANOVA, $p<0.05$). Differences were mainly caused by Mg:Ca, Mn:Ca, Co:Ca, Sr:Ca and Ba:Ca ratios (ANOVA, $p<0.05$). The Tukey's HSD shows that Mg:Ca ratio is significantly higher from eastern Mediterranean than the central or western Mediterranean. Mn:Ca and Co:Ca levels are significantly higher in samples from central Mediterranean comparing with the other areas (Tukey HSD $p<0.05$); Sr:Ca ratio differ between samples from eastern Mediterranean and western Mediterranean while Ba:Ca differs from western and central Mediterranean (Tukey HSD $p<0.05$) (Fig. 4.7). Results

from QDFA indicated that classification success for western, central and eastern Mediterranean was 80 %, 73% and 85% respectively.

The elemental analysis of otoliths allows the discrimination of Atlantic bluefin tuna from different nurseries within the Mediterranean Sea. In this study, the investigation was restricted to YOY bluefin tuna collected within the first six months of life. The chemical signature of bluefin tuna otoliths varied among the three nursery areas and the classification of samples was good for all the three groups giving strength to this approach as a valid tool to establish natal origin. Based on RF analyses, samples from western Mediterranean show a better classification rate (85%; Table 4.5). Otoliths from western Mediterranean are characterized by a lower value of Mg:Ca, Mn:Ca, Sr:Ca and Ba:Ca compared to otoliths from the other two nurseries, probably reflecting the different hydrography and trace element distribution from east to west Mediterranean basin. Our results indicate that Mg:Ca, Mn:Ca and Co:Ca are the variables that allow a good classification YOY bluefin tuna from central Mediterranean Sea, with a classification success of 73%. The higher values of Mn:Ca and Co:Ca significantly different compared to the other samples suggest the effect of hydrothermal activity or industrial input of that area on water composition and thus on otolith uptake. Otoliths from eastern Mediterranean shows a good classification (80%) due principally to the higher values of Mg:Ca in core signature. The significant difference of concentration of this micronutrient could be due to fluvial, anthropogenic or atmospheric inputs (dry and wet deposition, Saharan dust events) in the Levantine Basin. Furthermore the significantly higher concentration of Sr in otoliths from eastern Mediterranean Sea compared to those from western Mediterranean Sea, could reflect the salinity gradient across the Mediterranean basin.

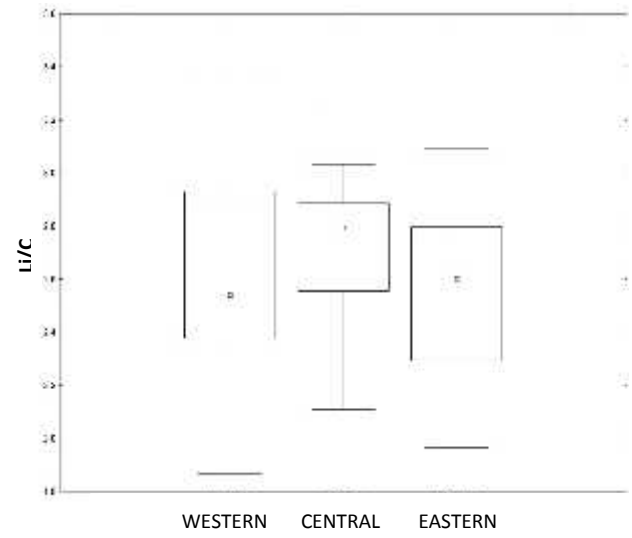
Li/C
WESTERN
CENTRAL
EASTERN

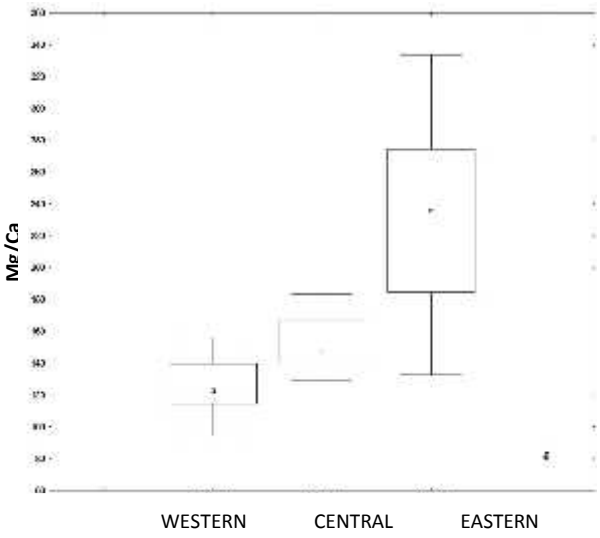
Mg/Ca
WESTERN
CENTRAL
EASTERN

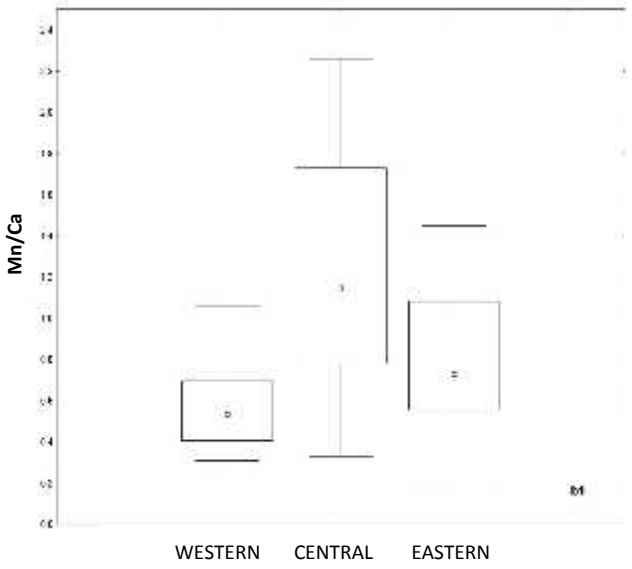
Mn/Ca
WESTERN
CENTRAL
EASTERN

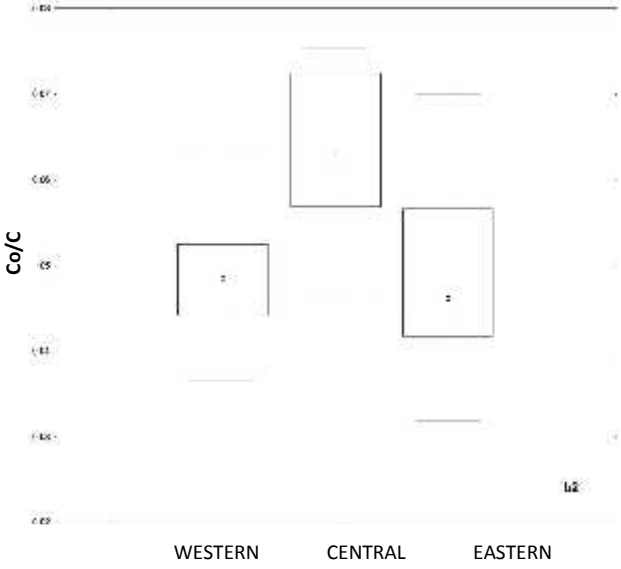
Co/C
WESTERN
CENTRAL
EASTERN

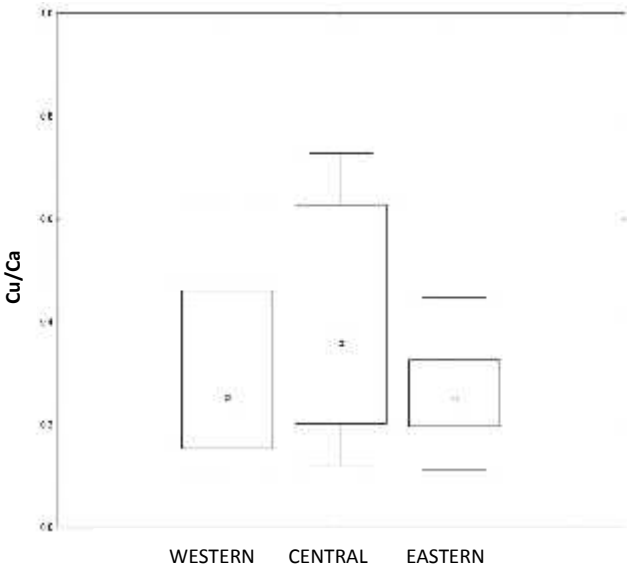
Cu/Ca
WESTERN
CENTRAL
EASTERN

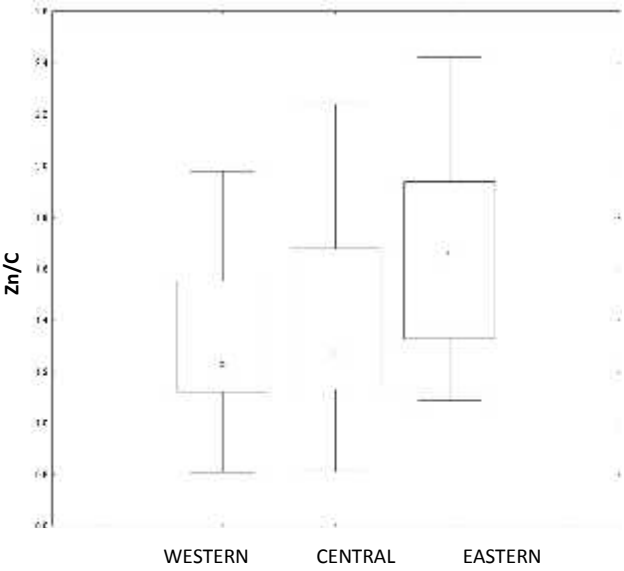
Zn/C
WESTERN
CENTRAL
EASTERN

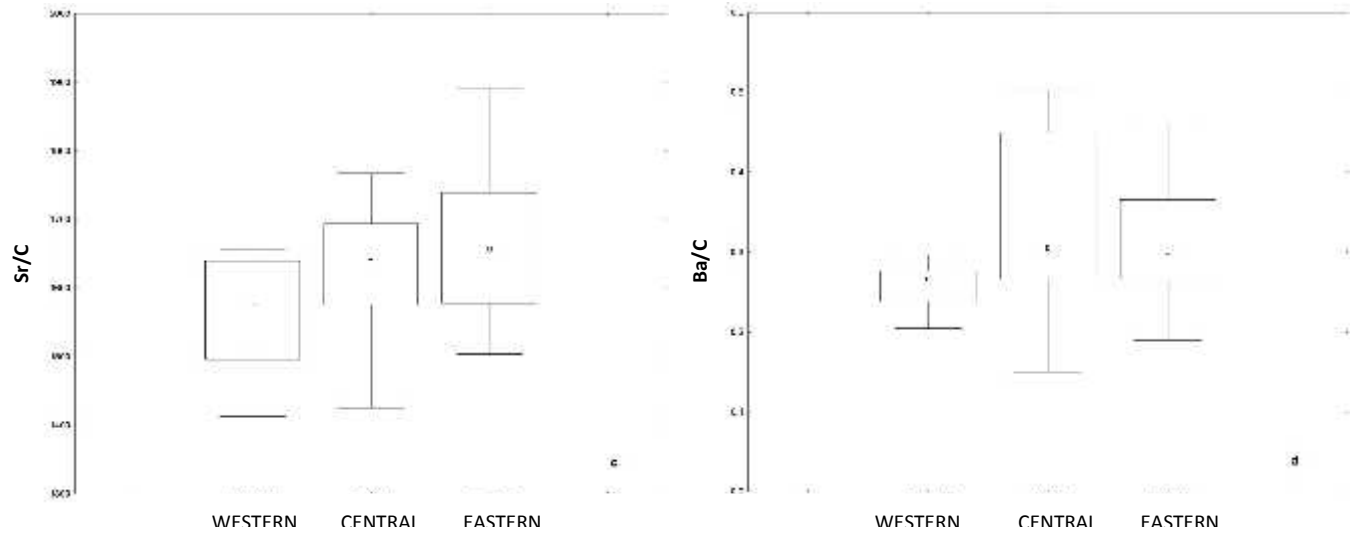

Figure 4.7: Box-plots comparing element:Ca distribution in otoliths of YOY bluefin tuna from western, central and eastern Mediterranean Sea. a: eastern Mediterranean significantly different from central and western Mediterranean ($p<0.05$). b1, b2: central Mediterranean significantly different from central and eastern Mediterranean ($p<0.05$). c: eastern Mediterranean significantly different from western Mediterranean ($p<0.05$). d: western Mediterranean significantly different from central Mediterranean ($p<0.05$).

Table 4.4: Information on sampling period and individuals of Atlantic bluefin tuna (Thunnus thynnus) within the Mediterranean Sea

Region	Year	N samples	Size Range (FL-mm)
Western Mediterranean	2012	20	340-370
Central Mediterranean	2012	20	350-400
Eastern Mediterranean	2012	20	200-460

Table 4.5: Classification success of YOY bluefin tuna from the western, central and eastern Mediterranean Sea estimated by Quadratic Discriminant Function Analysis (QDFA) and Random Forest (RF).

	% correct classification (QDFA)	% correct classification (RF)
Western M.	80%	85%
Central M.	73%	74%
Eastern M	85%	80%

In summary, the results of this study allow discrimination of YOY bluefin tuna from the three putative nursery areas based on their chemical composition. This study is a further contribution to previous investigations on nursery areas of bluefin tuna in the Mediterranean Sea (Rooker et al., 2003), and thus, to the study of population dynamics of this specie based on otoliths elemental analysis.

4.5. Determination of Atlantic bluefin tuna movements between Mediterranean Sea and western North Atlantic by $\delta^{13}C$ and $\delta^{18}O$ values along otolith transects

A new approach was tested with 10 bluefin tuna captured in the Bay of Biscay and Strait of Gibraltar by analyzing carbon and oxygen isotopes along a transect, from the central region of the otolith (representing early life history stages) until the edge of the otolith. Based on isotopic differences between Mediterranean Sea and Gulf of Mexico samples (see section 1 and Rooker et al., 2014), we assessed the utility of these two stable isotopes to detect if adult individuals captured in the eastern Atlantic Ocean have visited the western Atlantic throughout its lifetime.

Bluefin tuna used in this study were captured in July and August 2009 in the Bay of Biscay by the regional bait boat fleet, and during May 2010 by the Spanish traps located in Barbate. Bluefin tuna FL was measured to the nearest cm and otoliths were immediately extracted. Otolith handling followed the protocols previously described in Section 1, until the attachment to the sample plate. The milling of the otolith portion corresponding to each of the life stages was done using a New Wave Research MicroMill system. Transects of approximately 100 μm width were programmed to be perpendicular to the growth axis of the otolith (Fig. 4.8). Prior to otolith milling, a transect was milled on the epoxy resin along the otolith edge to avoid the inclusion of considerable amount of resin in the first otolith transect. Material from each of the portions was extracted using a drill path of a 300 μm diameter drill bit and 15 passes of 50 μm depth each. Powdered core material was transferred to silver capsules and later analyzed for $\delta^{13}C$ and $\delta^{18}O$ on an automated carbonate preparation device (KIEL-III) coupled to a gas-ratio mass spectrometer (Finnigan MAT 252). When milled powder was not enough for isotopic analyses, it was mixed with the material from the subsequent transect.

Figure 4.8: Photograph of an otolith transverse section showing the portions independently milled across the otolith growth axis

A total of 114 stable isotope analyses ($\delta^{13}C$ and $\delta^{18}O$) were carried on across the growth axis of 10 otoliths. In three of the selected otoliths from the Bay of Biscay we only were able to perform few transects after the yearling period (approximately 18 month). Based on the actual knowledge about bluefin tuna ecology we assume that during the yearling period bluefin tuna do not cross the entire Atlantic Ocean, and therefore these three otoliths were not further investigated. For the remaining otoliths a good number of transects were milled (Table 4.6), and the temporal evolution of $\delta^{13}C$ and $\delta^{18}O$ values was further explored.

Table 4.6: Summary data for the selection of otoliths from Atlantic bluefin tuna captured in the Bay of Biscay and Strait of Gibraltar. Total number of transects milled and analysed from the otolith edge to the otolith central region, and number of transects after of the yearling period (approximately after 18 month).

Otolith ID	Region	Age	Nº of transects	Nº of transects after 18m
AZTI-BB-J-538	Bay of Biscay	2	8	2
AZTI-BB-J-539	Bay of Biscay	2	8	3
AZTI-BB-J-540	Bay of Biscay	2	7	2
AZTI-BB-J-541	Bay of Biscay	3	14	8
AZTI-BB-M-181	Bay of Biscay	5	12	7
AZTI-BB-M-182	Bay of Biscay	5	11	8
AZTI-BB-M-183	Bay of Biscay	6	13	11
AZTI-BB-M-184	Bay of Biscay	6	11	8
AZTI-GI-L-1	Strait of Gibraltar	15	15	14
AZTI-GI-L-2	Strait of Gibraltar	14	15	15

Given that the discrimination of eastern and western populations is mostly based on differences in $\delta^{18}O$ values, we only focused in this variable to determine if individuals captured in the Bay of Biscay and Strait of Gibraltar have visited the western Atlantic Ocean throughout their lifetime. Using the baseline dataset, we estimated the lower limit of the 99% confidence interval for the eastern population $\delta^{18}O$ signature, which was of -1.4‰. Assuming that the signature of yearling individuals can be directly compared to juvenile and adult bluefin tuna (neglecting the effects of ontogeny on isotope incorporation into the otolith matrix), values below -1.4‰ were interpreted as possible migrations to the western Atlantic Ocean. Temporal variation in $\delta^{18}O$ signature of seven bluefin tuna has been represented against the growth axis of the otolith (Fig. 4.9). Time period covered varies among individuals, but in all cases the time frame from the 18 month (symbolized by the dashed line) to its capture is represented. Empty values are generated by the failure of the mass spectrometer (probably due to the lack of enough material).

During the yearling period (up to 18 month) the otoliths analyzed here reflect an initial increase of $\delta^{18}O$ followed by a gradual decrease around the age of 12 month. This pattern that repeats in all otoliths collected in the Bay of Biscay with sufficient transects within the yearling period, could be explained by the exit of bluefin tuna from the Mediterranean Sea towards the Atlantic Ocean, with more depleted values of surface water $\delta^{18}O$ compared to the Mediterranean Sea. After the yearling period, two of the five individuals captured in the Bay of Biscay could have visited the western Atlantic Ocean during their adolescence (AZTI-BB-M-181 and AZTI-BB-M-183), as their $\delta^{18}O$ values clearly cross the -1.4‰ boundary. The first individual, AZTI-BB-M-181 of age-5, could have inhabited in the open North Atlantic Ocean for several years, with successive visits to the western North Atlantic, before coming back to the eastern North Atlantic, were it was captured. Based on our results, the second bluefin tuna, AZTI-BB-M-183 of age-6, could have migrated twice to the western North Atlantic during its adolescence, and once again during the adult stage. However, $\delta^{18}O$ values on this individual are close to the -1.4‰ boundary, and present several blanks in the time series due to a technical failure. $\delta^{18}O$ signatures of both individuals captured in the Strait of Gibraltar (AZTI-GI-L-1 of age-15 and AZTI-GI-L-14 of age-14) may have resided in the western Atlantic Ocean during their adolescence, as both cross the -1.4‰ boundary.

However, one has to be cautious with the interpretation of these results, since the -1.4‰ boundary for $\delta^{18}O$ signature has been defined based on the reference database of yearling bluefin tuna, and the effects of ontogeny has not been taken into account.

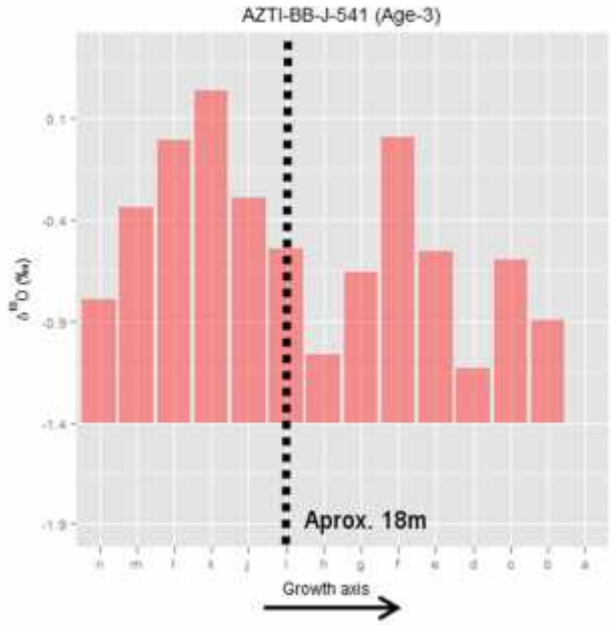
AZTI-BB-J-541 (Age-3)
Aprox. 18m
Growth axis

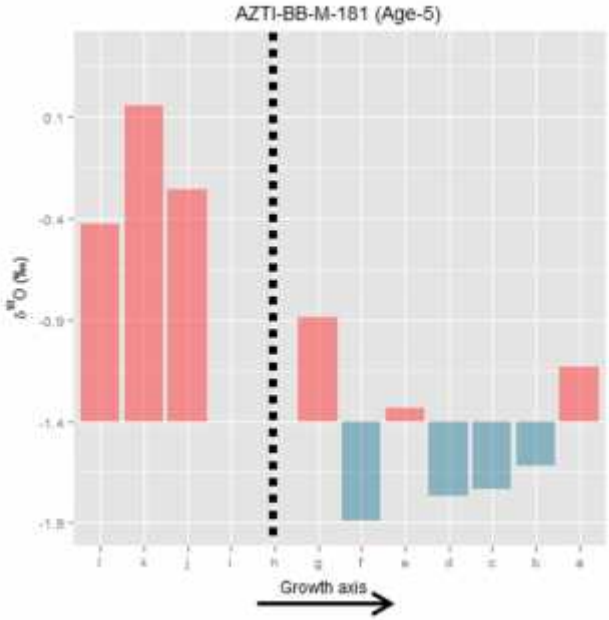
AZTI-BB-M-181 (Age-5)
Growth axis

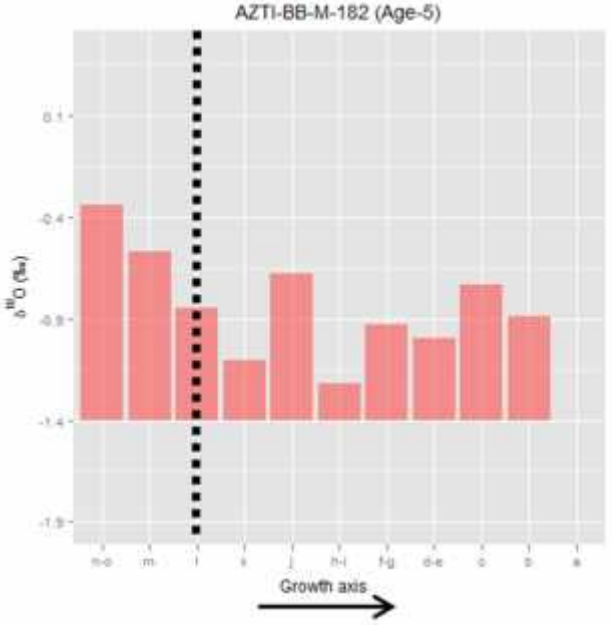
AZTI-BB-M-182 (Age-5)
Growth axis

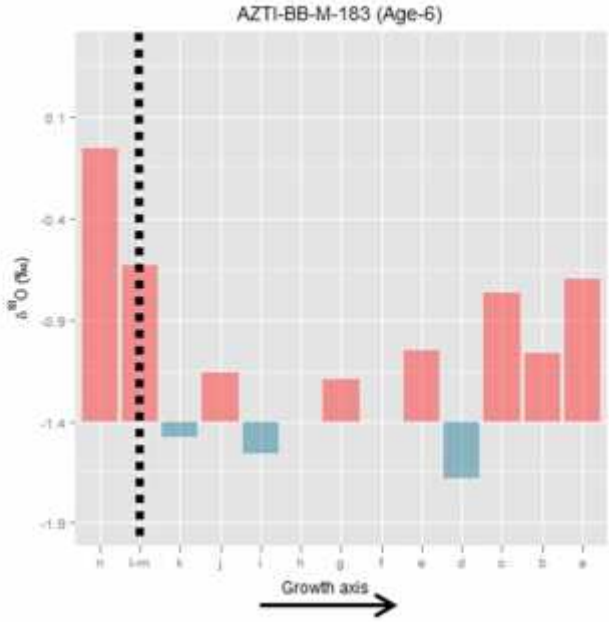
AZTI-BB-M-183 (Age-6)
Growth axis

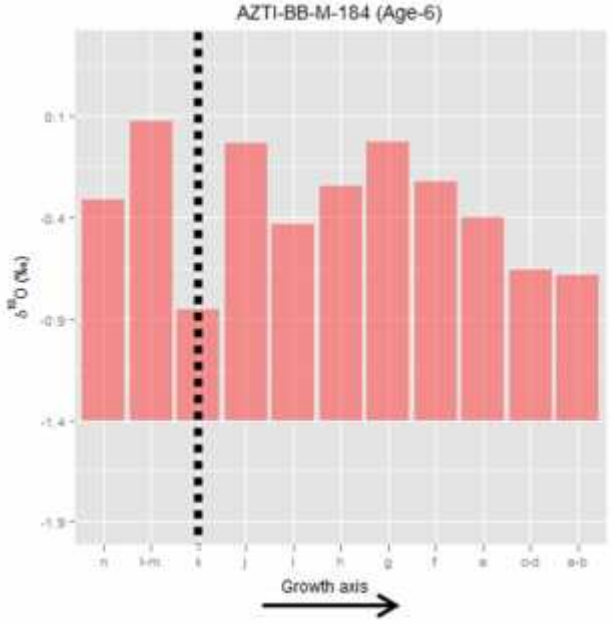
AZTI-BB-M-184 (Age-6)
Growth axis

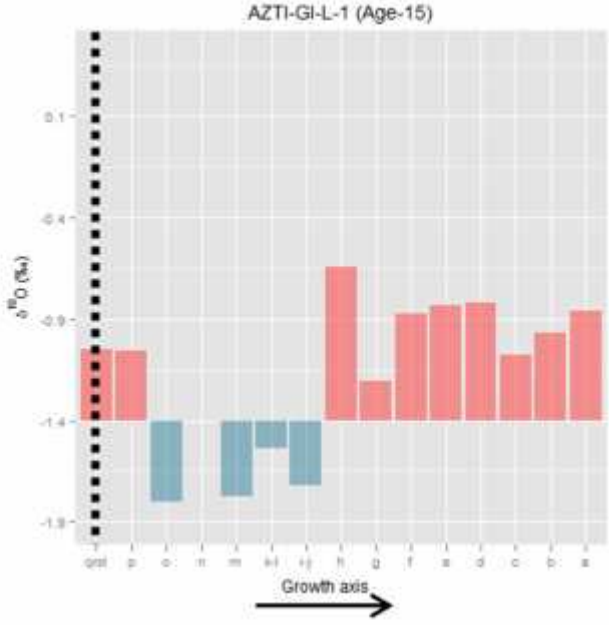
AZTI-GI-L-1 (Age-15)
Growth axis

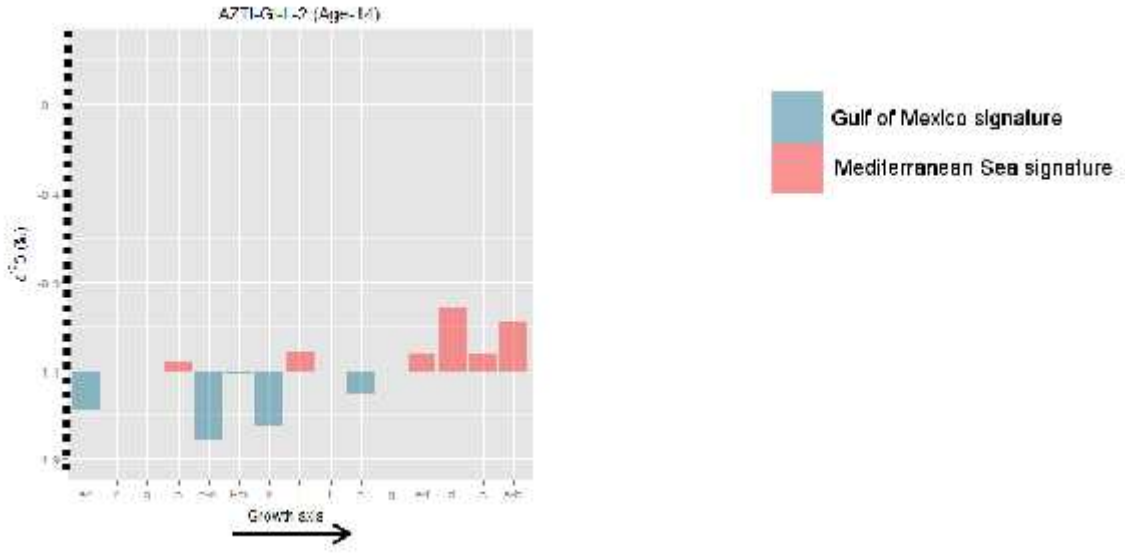

Figure 4.9: $\delta^{18}O$ values across the otolith transects in Atlantic bluefin tuna captured in the bay of Biscay (AZTI-BB-J-541, AZTI-BB-M-181, AZTI-BB-M-182, AZTI-BB-M-183 and AZTI-BB-M-184) and the Strait of Gibraltar (AZTI-GI-L-1 and AZTI-GI-L-2). Data represent different life stages throughout its lifetime, from the yearling period approximately at 18 month (the dashed line) until the time prior its capture. Each bar does not necessarily represent the same time length.

References

Breiman L (2001). Random forests. Machine Learning 45, 5-32.

Dickhut RM, AD Deshpande, A Cincinelli, MA Cochran, S Corsolini, RW Brill, DH Secor amd JE Graves (2009). Atlantic Bluefin Tuna (Thunnus thynnus) Population Dynamics Delineated by Organochlorine Tracers RID A-8468-2011. Environmental Science and Technology 43:8522-8527.

Fung, WK (1996). Diagnosing influentialobservations in quadratic discriminant analysis. Biometrics 52, 1235-1241.

Liaw A and Wiener M (2002). Classification and Regression by randomForest. R News 2, 18-22.

Miller, MB , AM Clough, JN Batson and RW Vachet, 2006. Transition metal binding to cod otolith proteins. Journal of Experimental Marine Biology and Ecology, 329, pp. 135–143.

Rooker JR, DH Secor, VS Zdanowicz, G DeMetrio, and LO Relini, 2003. Identification of northern
bluefin tuna stocks from putative nurseries in the Mediterranean Sea and western Atlantic Ocean using otolith chemistry. Fisheries Oceanography 12, 75-84.

Rooker JR, Alvarado Bremer JR, Block BA, Dewar H, De Metrio G, Kraus RT, Prince ED, Rodriquez-Marin E, Secor DH (2007) Life history and stock structure of Atlantic bluefin tuna (Thunnus thynnus). Reviews in Fisheries Science 15: 265-310

Rooker JR, Secor DH, DeMetrio G, Kaufman JA, Belmonte Rios A, Ticina A (2008a) Evidence of trans-Atlantic mixing and natal homing of bluefin tuna. Marine Ecology Progress Series 368: 231-239

Rooker JR, Secor DH, DeMetrio G, Schloesser R, Block BA, Neilson JD (2008b) Natal homing and connectivity in Atlantic bluefin tuna populations. Science 322: 742-744

Rooker, JR., Arrizabalaga H, Fraile I, Secor DH, Dettman DL, Abid N, Addis P, Deguara S, Karakulak FS, Kimoto A, Sakai O, Macías D, Neves Santos M (2014). Crossing the Line: Migratory and
Homing Behaviors of Atlantic Bluefin Tuna. Marine Ecology Progress Series 504, 265-276.

Schloesser RW, Rooker JR, Louchuoarn P, Neilson JD, Secor DH (2009) Interdecadal variation in seawater δ13C and δ18O recorded in fish otoliths. Limnology and Oceanography 54: 1665–1668

Schloesser RW, Neilson JD, Secor DH, Rooker JR (In press) Natal origin of Atlantic bluefin tuna (Thunnus thynnus) from the Gulf of St. Lawrence based on δ13C and δ18O in otoliths. Canadian Journal of Fisheries and Aquatic Sciences 67: 563–569.

Sturrock, AM , CN Trueman, AM Darnaude and E Hunter, 2012. Can otolith elemental chemistry retrospectively track migrations in fully marine fishes? Journal of Fish Biology 81, 766–795.

Watanabe, T., V Kiron and S Satoh, 1997. Trace minerals in fish nutrition. Aquaculture 151, 185–207.

5. GENETIC ANALYSIS OF ATLANTIC BLUEFIN TUNA USING NOVEL GENOMICS TOOLS

Task Leader: Fausto Tinti (UNIBO)

Participants

UNIBO: Gregory Neils Puncher, Alessia Cariani, Eleonora Pintus, Marco Stagioni, Fausto Tinti.

UPV-EHU: Andone Estonba, Aitor Albaina.

UNICA: Piero Addis, Rita Cannas.

Biogenomics-KULeuven: Gregory Maes, Koen Herten, Jeroen van Houdt.

IFREMER: Jean-Marc Fromentin.

AZTI: Naiara Rodriguez Ezpeleta, Urtzi Laconcha, Igaratza Fraile, Nicolas Goñi, Haritz Arrizabalaga.

5.1. Introduction

Single nucleotide polymorphisms (SNPs) have been used in several fisheries in recent years for various purposes such as determination of population structuring, traceability, hybridization rates and migratory dynamics (Nielsen et al. 2012; Albaina et al. 2013; Hess et al. 2014; Li et al. 2014; Houston et al. 2014; Larson et al. 2014). However, this new advance in population genetics has yet to be used for Atlantic bluefin tuna (BFT) conservation purposes. It has been the goal of the "Genetics" working group within GBYP to develop a high performance SNP panel capable of differentiating populations of BFT. The motivation to search for discriminatory SNPs within the BFT genome is a product of unresolved and often conflicting results from research that has used other molecular markers (ICCAT 2013). The ease by which data can be shared between research groups and the fact that SNPs can be sampled from throughout the entire genome, including genes influenced by selective pressures are additional benefits to this approach.

Originally, a dataset of individual genotypes for some 1328 BFTs, developed during GBYP Phase 3, was to be used for Phase 4 tasks (panel development and validation). However, due to the novel and innovative techniques used at the onset of the project (Reduced Representation Sequencing and Genotyping [RRSG/GBS] using the Illumina HiSeq2000), the quality of the data (insufficient and unequal distribution of read coverage) was unsuitable for the original tasks. After recognizing this issue, two new research pipelines were developed by the group and quickly launched. Using a reference genome, partially developed during GBYP Phase 2 and renovated several times since, as well as the RRSG data generated during GBYP Phase 3, partners at UNIBO and KULeuven's Biogenomics Core have combined the data from all individuals within 5 spawning areas and reanalyzed the data using a "Pooled data / Allele frequency approach". Meanwhile, partners at AZTI Tecnalia have extracted DNA from a subset of samples and utilized an entirely different NGS platform (Site Associated DNA sequencing or RAD-seq) in an effort to generate data from a completely different approach in order to validate the results of both pipelines.

5.2. Genotyping-by-Sequencing allele frequency analysis

Sequenced fragments of DNA extracted from larvae and young-of-the-year (reference strata), generated during GBYP Phase 3, have been pooled into 5 separate populations: Gulf of Mexico (GOM), Eastern Mediterranean (EM, Levantine Sea), Central Mediterranean (CM, Strait of Sicily), Western Mediterranean (WMBA, Balearic Sea), Ligurian Sea (WMLI) and Tyrrhenian Sea (WMTY). All fragments were trimmed using a new algorithm with an improved capacity for trimming away excess nucleotides (barcodes and adaptors) in the sequenced fragments, allowing for better overlapping of reads. Forward and reverse sequence reads were overlapped and quality checked and filtered using FLASH tools (Table 5.1).

Table 5.1. Fragments retained after filtration and quality check.

	% of data retained after demultiplex filtration	Number of reads
CM	87.36	135885940
EM	91.58	124845382
GOM	86.87	146942658
WMBA	90.09	225310444
WMLI	90.36	36418929
WMTY	86.88	282901496

These fragments were then aligned with a new and improved reference genome that has just recently been constructed by the KULeuven Biogenomics Core (Phase 4 Task 3). These small alterations to our approach have increased the amount of data available by as much as 30%, which translates into a higher number of correctly mapped fragments. Fragments with less than 50x read coverage were then discarded, resulting in retention of 866,121 fragments. FreeBayes software was then used for additional filtering steps using the same parameters as the human genome project: Mapping quality (>20 Phred Score) and Base quality (>15 Phred Score). The resulting .vcf file containing pooled data for each reference strata and 184.895 candidate loci was used for selection of high performance SNPs.

5.2.1 SNP selection

SNPs were selected based upon pairwise comparisons of all pooled groups and the difference between reference allele frequencies (delta value). A minimum read count per population of at least 18 was used as a threshold to maintain confidence in SNP validity. Preference was given for SNPs that had delta values between 1.0 and 0.7 (high), 0.7 and 0.6 (mid) and 0.6 and 0.5 (low). A total of 21 highly discriminatory SNPs, 63 mid, 100 low were selected for the panel (Table 5.2).

Table 5.2: Number of SNPs selected for the 384 trial SNP panel in order to differentiate between five spawning areas.

	GOM vs EM	GOM vs WMBA	GOM vs WMTY	GOM vs CM	EM vs WMBA	EM vs CM	EM vs WMTY	WMBA vs CM	WMTY vs CM	WMTY vs WMBA
High	8	4	0	2	1	14	9	9	1	5
Mid	7	9	0	3	1	19	8	19	1	12
Low	23	31	3	28	3	29	29	38	14	23
Total	**38**	**44**	**3**	**33**	**5**	**62**	**46**	**66**	**16**	**40**

The population from the Ligurian Sea had a very unique SNP composition in which they differed at many loci in an extreme manner from many populations. This being such, 78 SNPs were selected from pairwise comparisons between the Ligurian samples and other populations which had delta values higher than 0.995 and at least 50 read counts. Another 68 SNPs were selected from the same Ligurian pool with the same delta values and 30-49 read counts each. An additional 18 were selected for weak signals of discrimination (DV=0.5-0.38) between the Balearic Sea and the Levantine Sea. Likewise, 32 SNPs were with delta values of 0.4-0.38 were selected to increase the discriminatory power between the Levantine Sea and the Gulf of Mexico. Finally, 4 SNPs were selected for having the highest read depth across all populations. Although some of the SNPs selected may not prove useful for population assignment purposes, they will provide vital information necessary for other population genetic analyses that require neutral loci (HWE, minimum populations size, etc.). Task 1 of Phase 4 (Completing the bioinformatic processing and analyses of RRSG data obtained in previous GBYP Phases 2 and 3) has been achieved, in so far as analysis of RRSG/GBS data has been completed and 384 candidate SNPs capable of discriminating between populations have been selected for downstream applications.

5.2.2 SNP annotation

Using the SNP flanking regions derived from the improved reference genome, complete SNP-containing sequences have been compared to the genetic codes of sister taxa published in online databases (BLAST, Altschul et al. 1997), thereby fulfilling several

requirements from Phase 4 Task 3. From the 384 SNPs selected for additional Phase 4 activities, 73 were found to be significantly similar to published gene sequences. All sequence matches aligned with genes annotated for bony fish species, indicating a high level of sequencing accuracy. Of the 73 matches, only 2 sequences aligned with those from previously published BFT sequences, both of which were mitochondrial genes. This is an indication that a great deal of genomic investigation is still required for Thunnus thynnus. Among the aligned sequences are genes associated with metabolism, muscle and bone growth, immune response, embryonic and larval development, vision, muscle performance, body weight and fat and cell communication.

5.2.3 Future Work

The tasks of analysing the RRSG-derived dataset for population structure and feeding aggregate assignment, as well as the validation of selected SNP subpanel from RRSG data will be initiated upon delivery of the 384 SNP panel currently being manufactured by Fluidigm Corp. The SNP panel is expected to arrive by October 2014 and these two tasks could be accomplished by the end of 2014. The 188 samples (previously genotyped in Phase 3, Table 5.3) have been prepared (extraction and quality/quantity analysis) for SNP panel validation (the original proposal was for 192 individuals but due to the SNP panel design and the platform selected, it is necessary to include 4 blanks, or negative controls, within the panel). By genotyping these samples again the effectiveness of the RRSG/GBS and SNP panel selection pipeline will be determined.

Table 5.3: 188 samples selected for Phase 4 Task 3 SNP panel validation.

Region	Area	Year	Size class	Strata	Number of samples
WATL	GM	2008	0	WATL-GM-0-2008	16
WATL	GM	2007	V	WATL-GM-V-2007	5
WATL	GM	2008	V	WATL-GM-V-2008	5
WATL	GM	2009	V	WATL-GM-V-2009b	10
WATL	GM	2009	V	WATL-GM-V-2009	8
EMED	LS	2011	0	EMED-LS-0-2011	27
EMED	LS	2012	0	EMED-LS-0-2012b	21
CMED	SI	2011	0	CMED-SI-0-2011	21
CMED	SI	2012	0	CMED-SI-0-2012	27
WMED	BA	2011	0	WMED-BA-0-2011	24
WMED	TY	2012	0	WMED-TY-0-2012	24

During this process of validation, the most discriminatory or high performance SNPs will be selected and included in a reduced panel containing 96 - 192 SNPs, depending upon the results of the analysis. The purpose of this smaller panel will be to fulfill the remaining goals of Phase 4 Task 2, namely: i) discriminate between the Mediterranean spawning populations from the Gulf of Mexico, ii) differentiate the spawning populations within the Mediterranean, and iii) assess the spatial and temporal stability of the putative genetic clusters identified (since several replicates of the reference strata are available). Unfortunately, because of the way in which SNPs were chosen for the reduced panel (pooling data and selecting only the most discriminating loci) it may prove inappropriate for estimations of effective population sizes (Waples 2010).

Phase 4 Task 4 (Genotyping newly collected strata during GBYP-Phase4) is still to be achieved. Of course this cannot occur until after a reduced SNP panel has been developed in Task 3. The 576 samples to be used in Task 4 have already been ear marked (Table 5.4); however, the research group has allowed some flexibility in the pipeline in order to optimize the resulting deliverables in case one population or another displays characteristics of interest that require additional investigation.

Table 5.4: 576 samples selected for Task 4 genotyping of newly collected strata.

Region	Area	Year	Size class	Strata	Number of
EMED	LS	2011	L	EMED-LS-L-2011	30
CMED	AS	2011	J	CMED-AS-J-2011	30
CMED	MA	2011	L	CMED-MA-L-2011	30
CMED	SY	2012	M	CMED-SY-M-2012	30
WMED	GL	2011	J	WMED-GL-J-2011	15
WMED	LI	2011	J	WMED-LI-J-2011	15
WMED	SA	2011	L	WMED-SA-L-2011	30
WMED	TY	2011	M	WMED-TY-M-2011	30
NEAtl	BB	2011	J	NEAtl-BB-J-2011	30
NEAtl	CI	2013	L	NEAtl-CI-L-2013	30
NEAtl	GI	2011	L	NEAtl-GI-L-2011	15
NEAtl	MO	2012	L	NEAtl-MO-L-2012	30
NEAtl	MO	2013	L	NEAtl-MO-L-2013	30
NEAtl	PO	2011	L	NEAtl-PO-L-2011	15
CNAtl	CA	2011	M	CNAtl-CA-M-2011	30
CNAtl	CA	2012	M	CNAtl-CA-M-2012	25
CNAtl	CA	2011	L	CNAtl-CA-L-2011	30
CNAtl	CA	2012	L	CNAtl-CA-L-2012	30
NWAtl	GSL	?	L	NWAtl-GSL-L-?	15
NWAtl	NS	?	L	NWAtl-NS-L-?	15

While these newly collected strata are being genotyped using the reduced SNP panel, existing data from strata previously sequenced in Phase 3 will be re-analyzed and genotypes will be generated in silica for the corresponding 96-192 SNPs. Once all of this data is available the research group will be able to begin analysis of the feeding aggregates as defined in Phase 4 Task 2B. Several population assignment methods (e.g. GeneClass, Oncor, Structure, PCA approaches) with mix stock analysis techniques (e.g. cBayes, SPAM, Hwler) will be conducted and the results can be provided to the SCRS in early 2015.

5.3. RAD-Seq Approach

The RAD-seq method involves various steps: i) extraction of genomic good integrity DNA in enough quantity, ii) digestion of the genomic DNA by a restriction enzyme and ligation of complementary adaptors; iii) mechanical fragmentation and selection of fragments of a given size; iv) adaptor ligation and PCR amplification; v) sequencing.

5.3.1 Materials and Methods

RAD-seq libraries were constructed following the protocol from Etter et al. (2011) with some modifications and sequenced on the Illumina HiSeq platform. Obtained sequences have been checked for length and quality using FASTQC (http://www.bioinformatics.babraham.ac.uk/projects/fastqc/) and after ensuring adequate overall quality, sequences have been demultiplexed and trimmed using STACKS (http://creskolab.uoregon.edu/stacks/). The ustacks, csstacks, and sstacks modules of STACKS have been used for SNP discovery and genotyping based on the obtained RAD-tags. Further filtering has been performed with PLINK (http://pngu.mgh.harvard.edu/~purcell/plink/) and in-house developed scripts. Population structure has been assessed using Structure (http://pritchardlab.stanford.edu/structure.html).

5.3.2 Results

A total of 165 samples that yielded enough DNA for RAD-seq were selected, including larvae and young of the year (YOY) from the Gulf of Mexico, and Western, Central and Eastern Mediterranean (Table 5.5).

Table 5.5: Number of samples per location and age used for RAD-seq.

	Larvae	YOY	TOTAL
West Mediterranean	28	13	41
Gulf of Mexico	22	20	42
Central Mediterranean	22	20	42
Eastern Mediterranean	10	30	40
TOTAL	82	83	**165**

After sequencing quality check, 18 samples had to be rejected because of lack of enough sequences (threshold was set to 500,000 tags per sample). The average number of reads of the remaining samples was of 3,872,631 with a minimum of 615,154 and a maximum of 14,019,992 reads (Figure 5.1A). We obtained an average of 64956 tags (homologous unique fragment) per sample. Within these tags, an average of 22,952 alleles including 15,973 SNPs has been identified. The catalog including all samples comprised 1,506,880 tags to which an average of 64,495 tags per individual matched (Figure 5.1B).

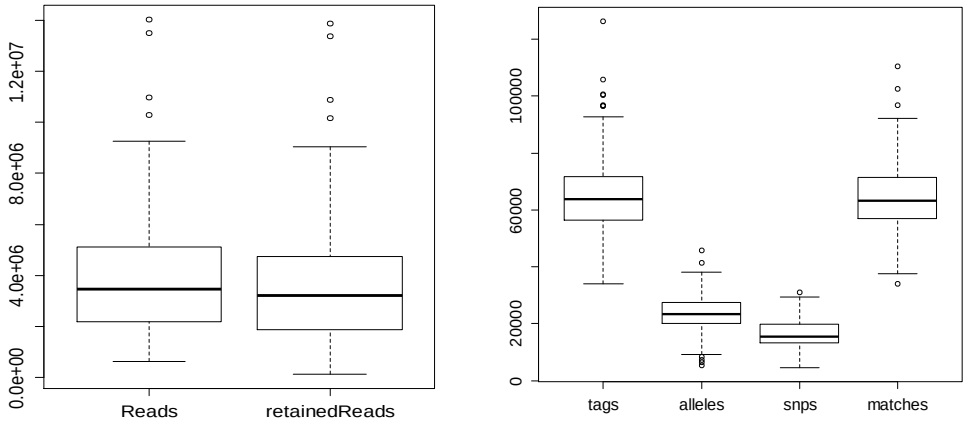

Figure 5.1. A: Boxplot showing total number of reads and reads retained for SNP discovery. B: Boxplot showing statistics of number of tags, alleles, SNPs and matches to the catalog.

The 1,506,880 tags included in the catalog were filtered to select only those present in at least 75% of the individuals. This lead to a total of 40,387 tags comprising 177,164 SNPs. These SNPs where filtered for minimum allele frequency (>0.05) and genotyping rate (>0.95). Individuals were also filtered for a genotyping rate of > 0.75. The final dataset contained 9,830 SNPs and 130 individuals.

The resulting dataset was analyzed using Structure for 100,000 generations with a burn in period of 10,000 (convergence was assessed by plotting the log likelihood values) under the admixture without location prior model. 10 replicates for each value of K were performed and the best K assessed using the Evanno method, which resulted in a best K of 4. The Structure plots (Figure 5.2) show a clear differentiation of the Gulf of Mexico samples from the Mediterranean samples. This difference is more pronounced in the case of larvae. Moreover a slight separation can be observed within the Meditterranean

sea, with the Western Mediterranean larvae being different from the rest of the sample. More analyses are still needed to confirm this hypothesis.

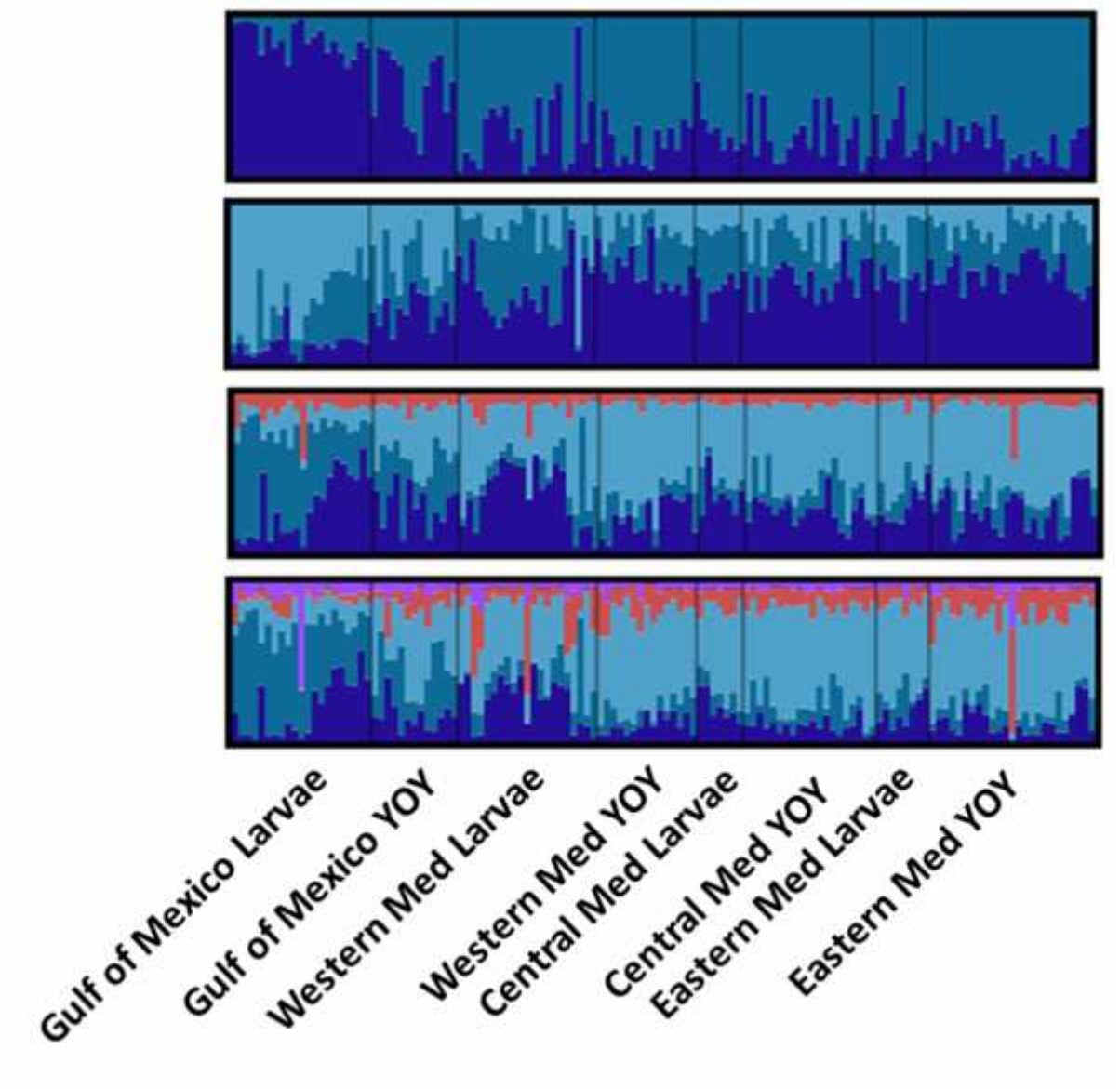

Figure 5.2. Graphic representation of individual ancestry using Structure software. Each bar represents one individual and each color, its degree of belonging to each inferred group.K varies from 2 to 5 from top to down.

Additionally, a DAPC analysis was performed using the R package adegenet. The clustering analysis shows a clear differentiation of the Gulf of Mexico individuals with respect to the other samples (Figure 5.3).

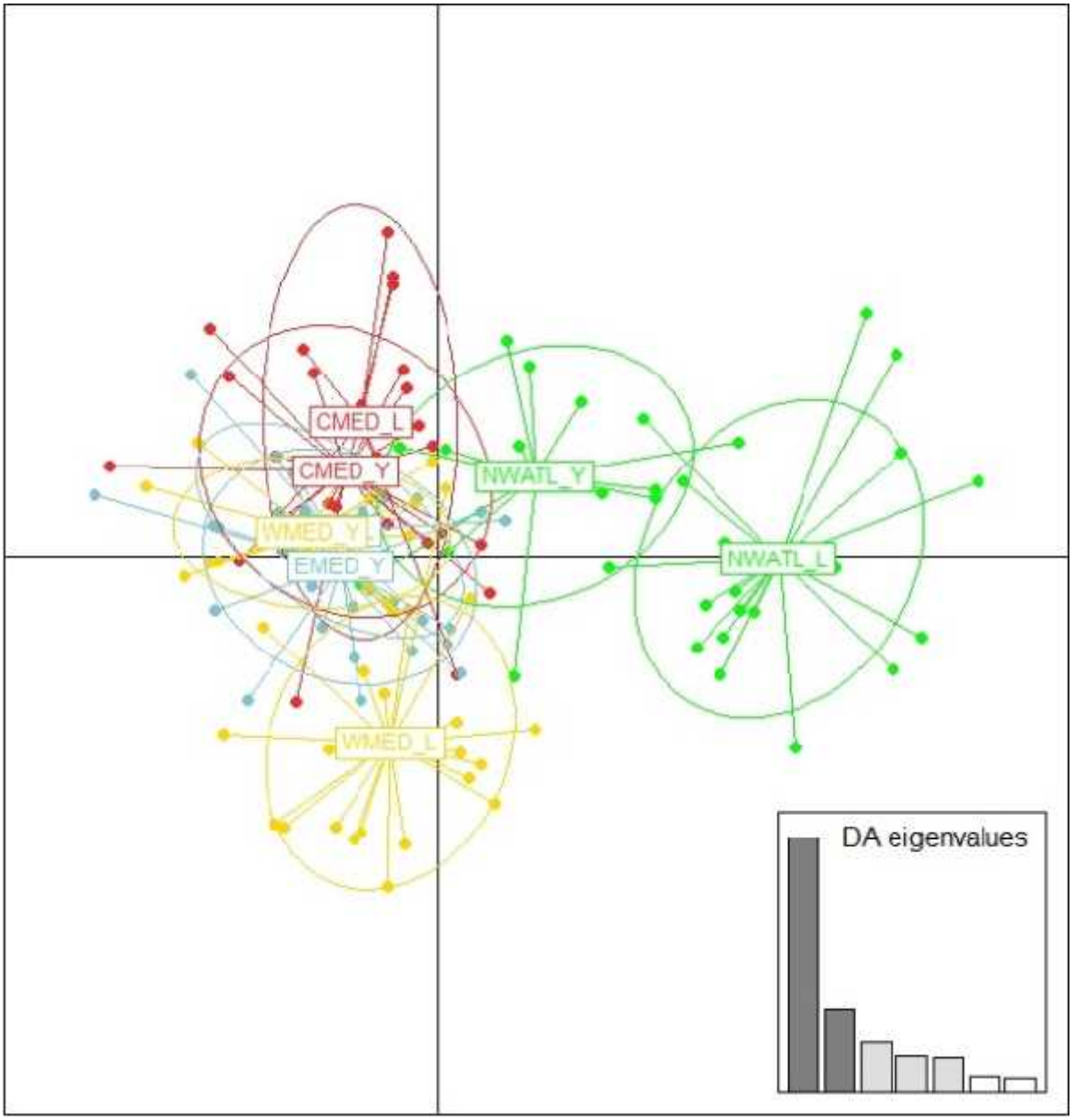

Figure 5.3. DAPC analysis of 130 samples assuming 8 distinct groups.

Ultimately, SNPs generated using the RAD-Seq approach will be combined with those from the RRSG approach in order to have the most effective high performance SNP panel possible.

References

Altschul, SF, Madden, TL, Schäffer, AA, Zhang J, Zhang, Z, Miller, W, and Lipman, DJ (1997). "Gapped BLAST and PSI-BLAST: a new generation of protein database search programs" Nucleic Acids Res. 25:3389-3402.

Etter, PD, Bassham, S, Hohenlohe, PA, Johnson EA and Cresko WA (2011). SNP Discovery and Genotyping for Evolutionary Genetics Using RAD Sequencing. Methods Mol Biol. 772: 157–178.

Houston, R.D., Taggart, J.B., Cézard, T., et al. (2014) Development and validation of a high density SNP genotyping array for Atlantic salmon (Salmo salar). BMC Genomics 15(1), 90.

ICCAT (2013) Report of the 2013 bluefin meeting on biological parameters review (Tenerife, Spain, 07 May – 13 May, 2013). pp. 1-75.

Larson, W.A., Seeb, L.W., Everett, M.V., Waples, R.K., Templin, W.D. and Seeb, J.E. (2014) Genotyping by sequencing resolves shallow population structure to inform conservation of Chinook salmon (Oncorhynchus tshawytscha). Evolutionary Applications 7(3), 355-369.

Waples R (2010). Perspective. High grading bias: subtle problems with assessing power of selected subsets of loci for population assignment. Molecular Ecology, 19, 2599–2601.

6. OTOLITH SHAPE ANALYSIS

Task leader: Deirdre Brophy (GMIT)

Participants:

GMIT: Deirdre Brophy, Paula Haynes

AZTI: Haritz Arrizabalaga, Igaratza Fraile

6.1. Summary

Summary

- There exists slight but significant spatial variation in otolith shape of bluefin tuna in the East Atlantic and Mediterranean (in feeding aggregations) which is independent of variation in size and is temporally consistent.
- There is a large degree of overlap in otolith shape between regions and fish can not be assigned to site of capture with acceptable levels of accuracy using otolith shape alone.
- The results indicate the existence of two groups that mix to varying degrees in the different regions during feeding.
- In adult bluefin otolith shape varies over broad spatial scales. Fish from the west Atlantic are the most distinct.
- Otolith shape may be useful for resolving underlying structure in Atlantic bluefin tuna, when combined with information from other methods (e.g. genetics, otolith chemistry) and ideally when applied to samples of known stock origin.

6.2. Introduction

Otolith shape is known to vary both between and within species (Lombarte and Castellon, 1991) due to the combined influence of genetic and environmental factors (Vignon and Morat 2012). Thanks to advances in image analysis, variation in otolith shape is now readily captured using geometric measurement of digitised otolith outlines (Stransky, 2013). Multivariate analysis of otolith shape data can be used to characterise fish from different stocks (Paul et al 2013) or to detect underlying structure in a mixed

assemblage of unknown stock composition (Keating et al 2014). The objective of this task was to extract otolith shape information from images of Atlantic bluefin tuna otoliths, to examine the extent to which shape varies spatially among feeding aggregations in the Atlantic and Mediterranean and to evaluate the usefulness of this method for resolving population structure in Atlantic bluefin tuna. Preliminary findings from this analysis are presented in this report.

6.3. Materials and methods

Sample details

Otoliths of Bluefin tuna collected in 2011-2013 from the eastern (Levantine Sea), western (Ligurian Sea, Gulf of Lyon, Gibraltar) and central (Adriatic Sea) Mediterranean, the northeast Atlantic (Bay of Biscay, Portugal, Morocco), Central North Atlantic and western Atlanic (Canada) were included in the shape analysis (Figure 6.1). From the available material up to 50 otoliths were randomly selected from each of three size strata (Juvenile <25kg, medium 25-100kg and large >100kg), for each area and year. Total lengths ranged from 55-178cm (Table 6.1).

Table 6.1: Summary details of bluefin tuna used in the analysis. Sample sizes are shown in italics; Mean total lengths (cm) are shown in regular type face, with ranges in parenthesis.

	2011			**2012**			**2013**			
Area	**Juvenile** (<25 kg)	**Medium** (25-100 kg)	**Large** (>100kg)	**Juvenile** (<25 kg)	**Medium** (25-100 kg)	**Large** (>100kg)	**Juvenile** (<25 kg)	**Medium** (25-100 kg)	**Large** (>100kg)	**Total N**
Adriatic (AS)	*18* 115.5 (109.8-122.2)	---		*32* 83.8 (76-104)	---		*48* 94.8 (79-110)	---		98
Bay of Biscay (BB)	*24* 71 (55-90.3)	*13* 127.4 (110-178)		*41* 62.8 (57.5-84)	*16* 127 (107-154.8)		*44* 70.5 (55.7-110)	---		*138*
Gibraltar (GI)	---	---	*3* 213.1 (190.7-250)	---	*22* 125.5 (110-175)	*29* 213.6 (183-260)	---	---		*54*
Gulf of Lyon (GL)	*9* 113.1 (104-119.4)	*16* 118.7 (112.3-126.9)		*25* 111.6 (102-130)	*16* 121.3 (111-144)		---	---		*66*
Levantine (LS)	---	*10* 154.1 (146-167)	*9* 203.8 (176-248)	---	*14* 144.2 (133-153)		---	---		*33*
Ligurian (LI)	*16* 96.5 (76-118)	*5* 123.8 (120-127)		*33* 103.1 (83-117)	*20* 144.2 (133-153)		---	---		*74*
Central North Atlantic (CA)						*33* 201.3 (165-222)				*33*
Morocco (MO)			*2* 230.5 (220-241)			*21* 209.9 (187-227)			*35* 215.1 (176-241)	*58*
Portugal (PO)			*16* 207 (183-235)			*41* 208.2 (180-281)				*57*
Malta (MA)			*26* 219.7 (197.7-261.7)			*51* 231.4 (184-283)				*77*
Canada (CD)									*30* 264.5 (220-297)	*30*
Grand Total										***718***

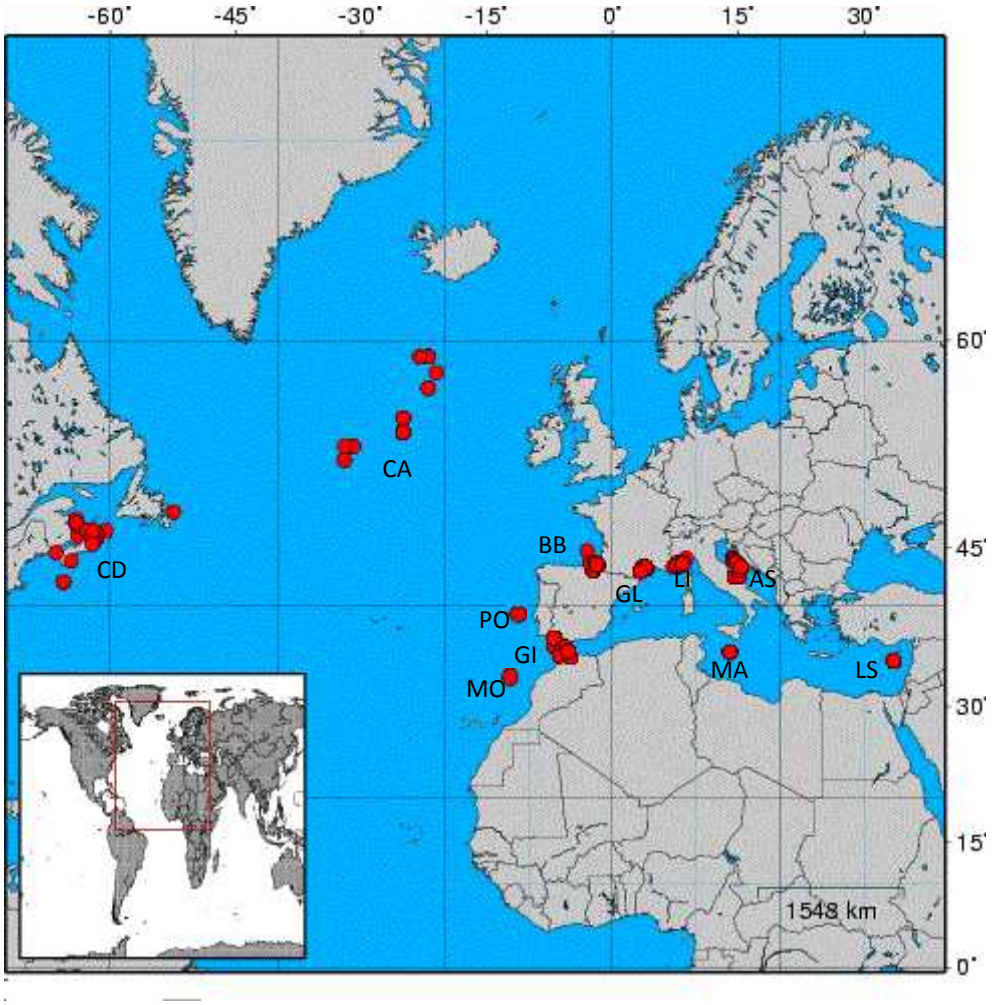

Figure 6.1: Map showing the sampling locations for the bluefin tuna (Thunnus thynnus) otoliths used in the shape analysis

Image capture and extraction of shape variables

Otolith images were captured using a stereomicroscope connected to a digital camera with a PC interface. Otoliths were photographed as a white object on a black background in a standard orientation, with the sulcus side uppermost and the rostrum pointing to left. The left otolith was used where possible. When the left otolith was unavailable the right otolith was photographed and the image was rotated. Otoliths were excluded from shape analysis when their outline was obscured by breakage or adhering dirt/tissue.

Otolith images were edited to standardise their orientation and to remove visual artefacts using Paint.NET v3.5.10. Using the ImageJ software package (available from http://rsb.info.nih.gov/ij/.n), a set of morphological shape indices was obtained from

physical measurements of each otolith image: circularity (4π x (area/perimeter2), aspect ratio (the ratio of the major and minor axes of the ellipse which binds the outline), roundness (4 x (π area/Major axis2) and solidity (area/convex area).

Using the TPSdig utility (*life.bio.sunysb.edu/morph/software.html*), images were converted to binary and otolith outlines were traced using edge detection and saved as a series of x-y co-ordinates. Elliptical fourier shape descriptors were extracted from smoothed otolith outlines using the momocs package in R. The optimal number of harmonics needed to capture the variation in the outlines was determined using a combination of visual inspection and the Fourier power equation (Crampton, 1995). Each harmonic is composed of 4 coefficients (an bn cn and dn). The first three coefficients of harmonic 1 (a1 b1 and c1) were used to standardise each outline for size, orientation and starting point.

Data analysis

The analysis was conducted in two stages. In the first stage, otoliths from the juvenile and medium size strata were used to investigate shape variation within the East Atlantic and Mediterranean. In the second stage shape variation was examined at a broader pan-Atlantic scale using otoliths from the large size stratum.

The shape of the otolith is under ontogenetic control and is known to change as a fish grows. Otolith shape could also vary from year to year within a region due to variation in the environment or the age structure of the population. These potential sources of variation could confound the interpretation of regional differences in otolith shape. The standardisation step included during the extraction of the fourier shape descriptors should remove any size related variation in otolith shape. The effectiveness of this standardisation process, and the possible influence of interannual variation was examined during the initial analysis of the data.

A series of ANCOVA's were conducted to determine if individual shape variables were correlated with fish length and differed significantly between regions and years. Year and region were included as a random and fixed factor respectively and total length was the covariate.

Variables that were significantly correlated with fish length and showed no heterogeneity in the size/shape relationship (length*region interaction, $p<0.05$) were standardised using the common within-group slope, according to the following equation:

$$Y_c = Y - b * L$$

Where Yc is the corrected variable, Y is the original variable, b is the common within group slope of the shape-size relationship (from ANCOVA), and L is the measurement of fish size (length).

Principal component analysis was conducted to reduce the dataset to a manageable number of uncorrelated descriptor variables that summarised the variability in otolith shape. The scree plot was used to identify the principal components that explained most of the variability in otolith shape. The selected principal components were then compared between regions and years using ANOVA and were used in a discriminant function analysis to classify fish to regions.

The bluefin used in this analysis were from feeding aggregations which are likely to contain mixtures of fish of different spawning origin. Therefore, groupings based on the region of capture may mask underlying structure in the data. Cluster analysis was conducted to determine if distinct otolith types could be identified from the principal components, with no a priori assumptions about their spatial distribution. The structure of the data was examined using hierarchial cluster analysis (Ward's linkage method; Minkwoski's distance metric). A k-means cluster analysis was then used to assign fish to clusters; the number of clusters was predefined based on the structure indicated by the hierarchical analysis.

Chi-square analysis was used to determine if cluster membership varied between samples and sample groups. In order to visualise the differences in otolith shape between clusters, average or median outlines were reconstructed by inverse fourier transform and plotted using the Nef-viewer program in Shape v 1.3 (Iwata and Ukai, 2002) and the efourier.shape function in momocs.

6.4. Results

One of the four shape indices (circularity) was found to vary significantly between regions (ANCOVA $p<0.05$) but not years (ANCOVA $p>0.05$). A significant correlation with fish length was detected which was effectively removed by standardisation using the common within-group slope.

Most of the fourier coefficients were found to vary significantly between regions (ANCOVA $p<0.05$) but not years (ANCOVA $p>0.05$). Some were correlated with fish length and so were corrected using the common within group slope. Coefficients were highly correlated with each other. The length corrected coefficients and circularity were included in the subsequent PCAs.

Analysis of juvenile and medium size strata (East Atlantic and Mediterranean)

The scree plot of Eigenvalues against principal components (PC's) indicated that principal components 1-5 effectively explained 81% of the variability in otolith shape. PC's 1, 2 and 3 showed small but significant variation between regions, and did not vary between years (Table 6.2).

Table 6.2: Results of ANOVA's comparing principal component scores between regions in the Eastern Atlantic and Mediterranean

Variable	R squared	F ratio	Sinificant pairwise comparisons (Tukey)
PC 1	0.049	4.1	BB v's AS and GL
PC 2	0.075	6.4	AS v's GL and LI; BB v's LI
PC 3	0.104	9.2	AS v's LI and LS; BB v's GI, GL and LI

A stepwise discriminant function analysis based on PC's 1, 2 and 3 was statistically significant (Wilk's Lambda= 0.78, $p<0.001$). However, the canonical scores plot showed extensive overlap between regions (Figure 6.2) and the Jacknife classification matrix indicated that the discriminatory power of the principal components in assigning fish to regions was weak (Table 6.3). For three regions (Adriatic Sea, Bay of Biscay and Ligurian Sea) fish were classified to regions with an accuracy rate approximately twice the rate expected by chance alone (i.e. 100/6 = 17%). For the remaining regions (Gibraltar, Gulf of Lyon, Ligurian Sea) classification rates were lower than expected by chance alone.

Table 6.3: Jacknife classification matrix from the discriminant function analysis (juvenile and medium size strata), using PC's 1, 2 and 3 to discriminate between bluefin from the six sampling regions.

AS	35	21	12	8	8	7	38
BB	36	48	10	4	26	9	36
GI	5	2	2	3	5	4	10
GL	8	9	18	7	17	2	11
LI	9	10	11	7	25	8	36
LS	4	6	6	1	5	2	8
Total	97	96	59	30	86	32	30

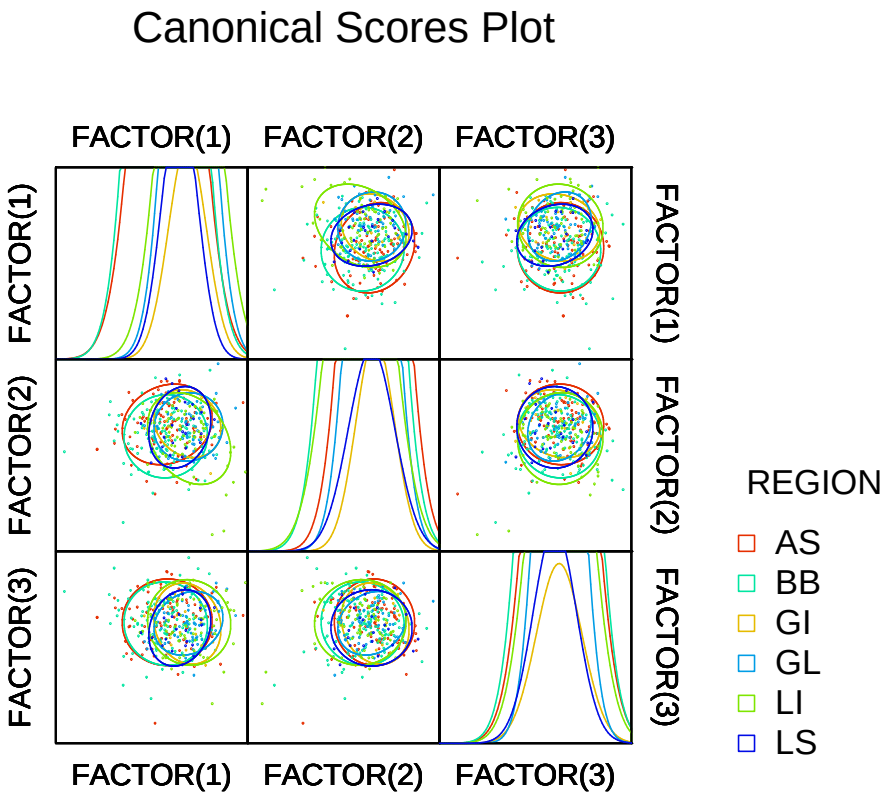

Figure 6.2: Canonical scores plot from the discriminant function analysis (juvenile and medium size strata), using PC's 1, 2 and 3 to discriminate between bluefin from the six sampling regions.

The cluster analysis indicated the presence of two clusters in the data (Figure 6.3). The exact composition of each cluster varied depending on the method used (hierarchical or K-means) and the combination of PC's used in the analysis (PC's 1, 2 and 3 only; PC's 1-5). However, a consistent pattern emerged in the mean outline of the two clusters and the spatial distribution of the clusters. The main difference in the shape of the otoliths within the two clusters appeared to be in the depth of the cleft between the rostrum and antirostrum and the width of the posterior end of the otolith relative to its length (Figure 6.4). Cluster two was more abundant than cluster one at most sites. Samples collected from the Bay of Biscay contained the highest proportion of fish from cluster 2 (75%) while samples from Gibraltar contained the lowest (47%) (Table 6.4). Chi-square analysis confirmed that the difference in the proportions of the two clusters between regions was significant (Chi square statistic: 16.8; $p<0.005$).

Table 6.4: Relative proportions of the two clusters in samples from each of the six regions

Region	% Cluster 1	% Cluster 2
AS	47.3	52.7
BB	24.1	75.9
GI	52.4	47.6
GL	42.6	57.4
LI	37.1	62.9
LS	41.7	58.3

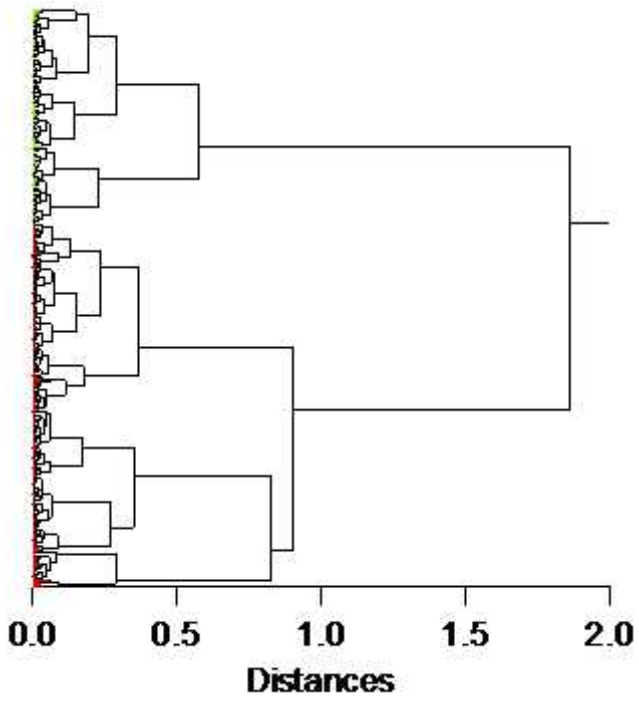

Figure 6.3: Cluster tree from a hierarchial analysis (Ward's linkage method) of principal components 1-5. Distances are calculated using the Minkowski metric.

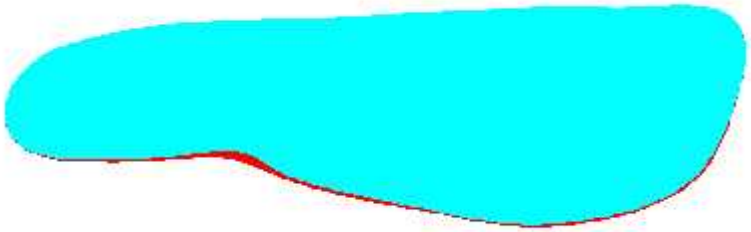

Figure 6.4: Silhouettes representing the mean outline described by the first 12 elliptical fourier harmonics for otoliths in cluster 1 (red) and cluster 2 (blue).

Analysis of large size stratum (Pan-Atlantic comparison)

For this analysis two sample groupings were considered. Firstly shape measurements were compared between the 7 capture ocations (CA, CD, GI, LS, MA, MO and PO). Samples were then grouped according to their likely nursery origin as indicated by otolith stable isotope signatures of bluefin from the same areas (Schloesser et al 2010; Rooker et al 2014). Samples from Canada (CD) were assumed to be predominantly of western origin (WEST) while samples from the Eastern Atlantic and Mediterranean (GI, LS, MA, MO, PO) were assumed to be of eastern origin (EAST). Aggregations of bluefin in the central north Atlantic have been shown to contain a mixture of eastern and western origin fish, with relative proportions varying annually. Therefore fish from this area (CA) were placed in a third category (MIXED).

Principal components 1-10 explained 67% of the variability in otolith shape. PC's 1, 4 and 6 and 9 showed small but significant variation between groups (Table 6.5). PC's 9 and 6 also showed annual variation at the locations that were sampled in multiple years (PO, MO, MA).

Table 6.5: Results of ANOVA's comparing principal component scores between sampling locations and between nursery origin groupings

Variable	R squared	F ratio	Significant pairwise comparisons (Tukey)
Sample location comparison			
PC 1	4.1	3.1	CA>CD; MA>CD;
PC 4	4.7	3.4	CA<MA
PC 6	2.7	2.4	CD<GI,MO,PO
PC 9	3.4	2.7	MO>GI; PO>GI;
Likely nursery origin comparison			
PC 1	4.3	7.7	EAST>WEST
PC 4	2.7	5.1	EAST>MIXED
PC 6	2.5	4.9	EAST>WEST

A stepwise discriminant function analysis based on PC's 1, 4 and 6 was used to classify fish according to assumed nursery origin (EAST, WEST and MIXED). The model was statistically significant (Wilk's Lambda= 0.89, $p<0.001$). The canonical scores plot showed some separation of the groups but with considerable overlap (Figure 6.5). The Jacknife classification matrix showed that correct classification rates were highest for the WEST group (70%; Table 6.6).

Table 6.6: Jacknife classification matrix from the discriminant function analysis (large size stratum), using PC's 1, 4 and 6 to discriminate between bluefin according to assumed nursery origin.

EAST	103	66	66	44
MIXED	10	18	6	53
WEST	5	4	21	70
Total	118	88	93	47

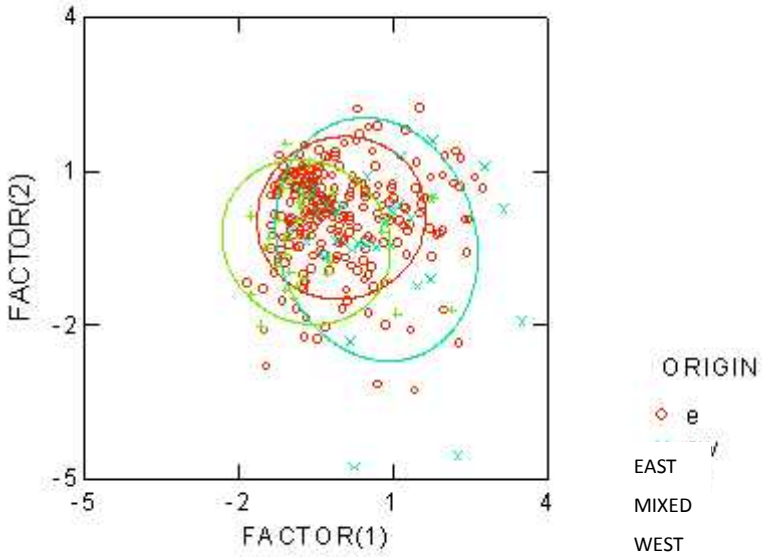

Figure 6.5: Canonical scores plot from the discriminant function analysis (large size stratum), using PC's 1, 4 and 6 to discriminate bluefin according to assumed nursery origin.

The cluster analysis indicated the presence of two clusters in the data (Figure 6.6). Samples assumed to be of predominantly western origin contained a higher than expected proportion of "cluster 2" otoliths; samples of assumed mixed origin contained a higher than expected proportion of "cluster 1" otoliths while the proportion of the two clusters were distributed in proportion to their numerical abundance in samples of

eastern origin (table 6.7). Chi-square analysis confirmed that the difference in the proportions of the two clusters between groups was significant (Chi square statistic: 15.2; $p<0.001$).

Table 6.7: Relative proportions of the two clusters in samples grouped according to assumed nursery origin groups (large fish analysis).

Group	% Cluster 1	% Cluster 2
EAST	65.5	34.5
MIXED	41.2	58.9
WEST	86.7	13.3

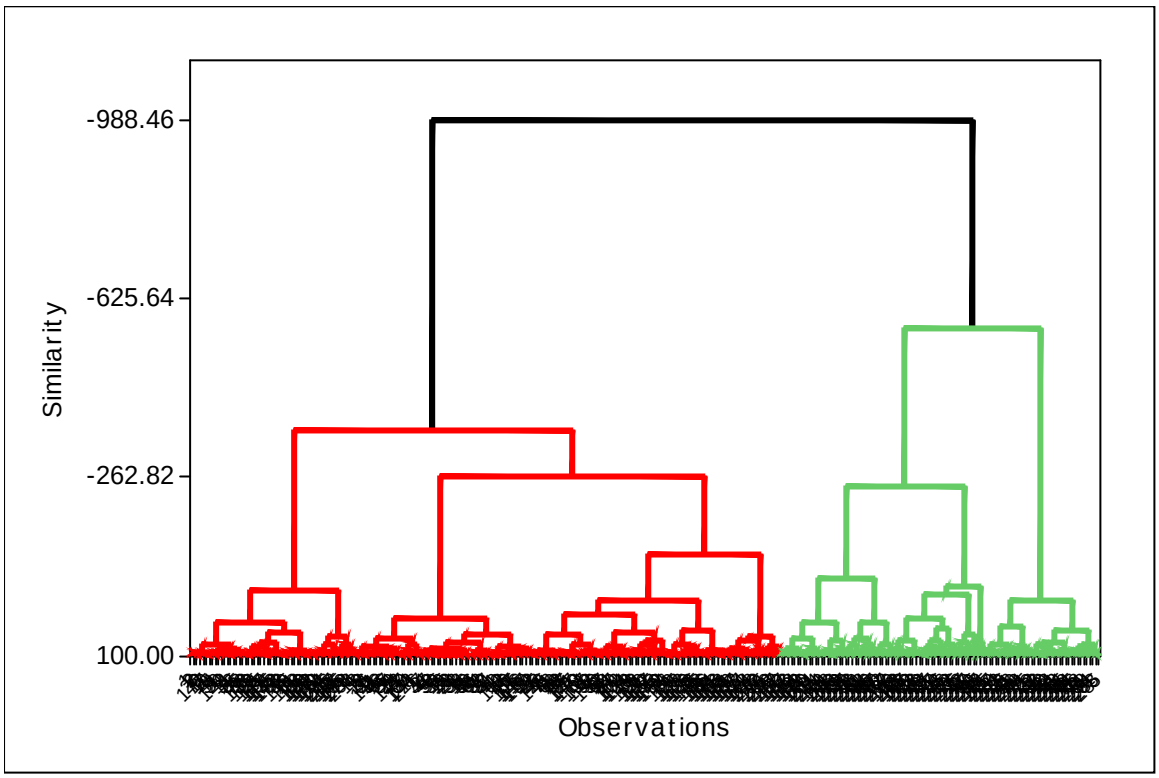

Figure 6.6: Cluster tree from a hierarchial analysis (Ward's linkage method) of principal components 1, 4 and 6 (large fish stratum). Distances are calculated using the Manhattan metric.

6.5. Discussion

Juvenile/medium analysis

The analysis of the juvenile and medium size strata revealed subtle but significant spatial variation in otolith shape of bluefin tuna which is independent of variation in size and appears to be consistent across the three years of sampling. Although the shape data could not be used to classify fish to site of capture with acceptable levels of accuracy, the fact that some variation is detected indicates that fish from the six regions examined do not form a homogenous group. Characterisation of regions could be improved by combining the otolith shape data with the outputs from the otolith chemistry and genetic analyses.

The results of the cluster analysis suggests that the samples may contain two groups, with relative proportions of the two groups differing between the six regions. This may reflect the presence of more than one spawning population in the area which mix to

varying degrees in different parts of the feeding aggregations. Alternatively variation in shape could arise if components within a single spawning population follow distinct migration pathways. By combining the otolith shape data with information on the genetics of the fish and chemical composition across the otolith trajectory these two possibilities could be further explored.

Large fish analysis

Despite the broader geographical coverage of sampling for the large size category the amount of otolith shape variation that could be explained by sampling origin was low. This is not surprising given the highly migratory nature of the species. Tagging studies show that fish occurring at the same location at one point in time may have very different environmental histories due to divergent migrations (Stokesbury et al, 2005).

Otolith shape is driven by the combined influence of genetic and environmental factors integrated over the whole life of the fish. Variation in otolith shape may not necessarily indicate that groups are of distinct stock origin. Nonetheless, the observed variation in otolith shape between samples appeared to be to some extent related to the likely stock composition of the samples. Although all groups overlapped, bluefin of western origin were the most distinct in terms of otolith shape. The limitations of the approach taken must be acknowledged; the actual stock composition of each sample was not known and may have varied from previous observations, particularly for the central North Atlantic. Sample sizes were limited for some areas and the western stock was more than likely poorly represented.

An inherent difficulty in the analysis is the lack of baseline samples of known stock origin. Ideally, spawning populations would be characterised using otoliths from spawning adults, allowing the stock composition of mixed samples to be determined. Although young of the year (YOY) are also likely to originate from the area in which they are caught, the shape of their otoliths would be quite distinct to that of older fish due to the ontogenetic component of otolith shape. Sampling of spawning adult bluefin tuna is difficult and opportunistic. However, even a small number of reference otoliths would provide a useful comparison with the otolith types observed here and would greatly enhance the resolving power of the otolith shape analysis. It is recommended that the capture of images from clean unbroken otoliths is included in the sampling

protocol in the future to maximise the amount of information obtained for investigation of stock structure.

References

Crampton, J.S., 1995. Elliptic Fourier shape analysis of fossil bivalves: some practical considerations. Lethaia 28, 179–186.

Fromentin J.M., 2009. Lessons from the past: investigating historical data from bluefin tuna fisheries. Fish and Fisheries 10, 197-216

Iwata, H., Ukai, Y., 2002. Shape: a computer based package for quantitative evaluation of biological shapes based on elliptic Fourier descriptors. Journal of Heredity 93, 84–385.

Keating, J.P., Brophy, D., Officer, R.A., Mullins, E., 2014. Otolith shape analysis of blue whiting suggests a complex stock structure at their spawning grounds in the Northeast Atlantic. Fisheries Research 157, 1–6

Lombarte, A., Castellón, A., 1991. Interspecific and intraspecific otolith variability in the genus Merluccius as determined by image analysis. Canadian Journal of Zoology 69, 2442–2449.

Paul, K., Oeberst, R., Hammer, C., 2013. Evaluation of otolith shape analysis as a tool for discriminating adults of Baltic cod stocks. Journal of Applied Ichthyology 29, 743–750.

Rooker, J., Arrizabalaga, H., Fraile, I., Secor D. H., Dettman D. L., Abid N., Addis P., Deguara S., Karakulak F. S., Kimoto A., Sakai O., Macías D., Neves Santos M. 2014. Crossing the line: migratory and homing behaviors of Atlantic bluefin tuna. Marine Ecology Progress Series, 504, 265-276.

Schloesser, R.W., J.D. Neilson, D.H. Secor, and J.R. Rooker. 2010. Natal origin of Atlantic bluefin tuna (Thunnus thynnus) from Canadian waters based on otolith δ13C and δ18O. Canadian Journal of Fisheries and Aquatic Sciences, 67:563-569. DOI:10.1139/F10-005.

Stransky, C., 2013. Morphometric Outlines. In Stock Identification Methods: Applications in Fishery Science Second Edition. Editors Steven X. Cadrin, Lisa A. Kerr, Stefano Mariani Published by Elsevier.

Stokesbury, MJW; Cosgrove, R; Boustany, A; Browne, D; Teo, SLH; O'Dor, RK; Block, BA. 2007. Results of satellite tagging of Atlantic bluefin tuna, Thunnus thynnus, off the coast of Ireland. Hydrobiologia 582:91–97.

Vignon, M., Morat, F., 2010. Environmental and genetic determinant of otolith shape revealed by a non-indigenous tropical fish. Marine Ecology Progress Series 411, 231–241.

7. CALIBRATION EXERCISE IN COLLABORATION WITH GBYP COORDINATION

Task leader: Enrique Rodríguez-Marín (IEO)

Participants:

GBYP COORDINATOR: Antonio Di Natale

IEO: Pablo Quelle, Marta Ruiz.

CSIRO: Jessica Farley

Gulf Coast Research Laboratory: Patricia Lastra Luque

Hellenic Centre for Marine Research: George Tserpes

IRD/IFREMER/UM2: Fany Sardenne

NOAA: Robert Allman, Ashley Pacicco

NRIFSF: Taiki Ishihara

SABS: Dheeraj Busawon

UNIBO: Marco Stagioni, Ennio Russo

UNICA: Andrea Bellodi, Stefania Vittori

UNIGE: Fulvio Garibaldi, Luca Lanteri, Alessandro Marcone

University of Athens: Persefoni Megalofonou, Niki Milatou

University of Maine/Gulf of Maine Research Institute: Elise Koob

7.1. Introduction

Currently, catch at age of Atlantic bluefin tuna (Thunnus thynnus) is generated by age slicing, a technique that divides catch length into different ages using a deterministic growth model, by separating size distributions into age classes under the assumption that there are distinct lengths which separate adjacent age classes. Given the variability in growth between individuals, which increases as fish grows, this technique can assign an incorrect age when one or more ages classes overlaps in length. This can be more critical in proportions of the older ages, where there is considerable overlap in length-at-

age. Growth variability over time and strong cohorts signal can also be affected by this deterministic method (Kell and Ortiz, 2011).

Direct ageing may reduce this uncertainty and results in more reliable catches at age, providing more robust stock assessment models. But standardization of direct ageing and quality control is needed before applying direct ageing to create catch at age matrix for any species (Campana, 2001). In this regard, considerable progress has been made in bluefin tuna direct ageing in recent years by using the two most commonly calcified structures (CSs) employed to age this species: otoliths and first rays of the first dorsal fin (spines). Age determinations from otoliths have been validated, age interpretation protocols have been established for spines and are being developed for otoliths, and inter-calibration experiences are being carried out among laboratories for both structures, including age interpretation from paired structures coming from the same specimens (Neilson and Campana, 2008; Rodriguez-Marin et al., 2013; ICCAT 2013; Busawon et al., 2014; Luque et al., 2014).

The use of digital images is an established procedure and image analysis systems can improve discrimination of growth bands. Digital images facilitate exchange exercises of CSs among laboratories easing the exchange speed, since images are available for all participants at the same time. The lack of standardized interpretation procedure for otoliths together with the shortage of laboratories that are currently conducting direct ageing for this species, particularly using spines for age interpretation, require a calibration exercise where the variables that may influence the ability to age are properly identified. With this objective and to assess the use of calcified structures for obtaining age composition of bluefin tuna catches, an ageing calibration exercise in collaboration with GBYP Coordination was launched. This report presents the analysis of the results.

7.2. Material and Methods

A set of digital images of sections of paired CSs, otoliths and spines, coming from the same specimen was prepared. All images had a scale bar for magnification reference and used Tiff-format to allow adding raster layers for: 1- a specific scale bar layer for first annulus identification in otoliths, 2- an image enhancement layer and 3- a layer for each reader age annotations. Three sets of images were prepared: otoliths with transmitted

(OT) and reflected light (OR) and spines with transmitted light (ST). Samples were selected by length classes, targeting a minimum of 3 specimens by 10 cm length class for an overall total of 100 specimens (three sets of 100 images).

A call to participate in this exchange was announced on ICCAT main web page. Participants were asked to provide information about their reading experience. A set of documentation was available for the participants: instructions and recommendations, a compilation of bluefin tuna direct ageing references and available age interpretation criteria for both CSs and a brief report with the preparation methods used to obtain the digital images of the exchange. A reading form was established with relevant information for the age interpretation of each type of CS.

The exchange results were analyzed testing for significant differences in age reading methods, among age readers and to test whether different CSs cause significant differences in age reading results. A combination of statistic, using the coefficient of variation (CV), the average per cent error (APE) and the relative bias with respect to the modal age, and age bias graphs, were used as tools to evaluate the precision, relative accuracy and agreement (Campana et al., 1995; Eltink et al., 2000).

7.3. Results and Discussion

Exchange participation

The ICCAT call for expressions of interest to participate in the exchange had a big success with 34 scientist responses, coming from 16 institutions and 10 countries. The number of age readers that sent their readings and annotated images within the deadline reached 62% of the total and some other readings are expected in the first week of September. These results are quite good considering the limited time available for the exchange, three months, and the coincidence with vacation period. Table 7.1 shows the list of participants describing their reading experience by CS.

Table 7.1 Participants in the calibration exercise and their experience in age estimation on bluefin tuna by calcified structure (exp= experienced, inexp= inexperienced).

Institution	Participants	Reader coding	Reading experience	
			Otoliths	Spines
Instituto Español de Oceanografia - Santander (Spain)	Enrique Rodiguez-Marin	ERM	exp	exp
	Marta Ruiz Sobrón	MRS	inexp	exp
	Pablo Quelle Eijo	PQE	inexp	inexp
Laboratorio di Biologia Marina e Pesca dell'Università di Bologna - Fano (Italy)	Marco Stagioni	MST	inexp	inexp
	Ennio Russo	ERU	inexp	inexp
Department of Environmental Life and Science, University of Cagliari (Italy)	Andrea Bellodi	ABE	exp	inexp
	Stefania Vittori	SVI	exp	inexp
Department of Biology, University of Athens (Greece)	Persefoni Megalofonou	PME	exp	exp
	Niki Milatou	NMI	inexp	exp
Dipartimento di Scienze della Terra, dell'Ambiente e della Vita, University of Genova (Italy)	Fulvio Garibaldi	FGA	exp	exp
	Luca Lanteri	LLA	exp	exp
	Alessandro Marcone	AMA	inexp	inexp
NOAA, Southeast Fisheries Science Center, Panama City Laboratory, Panama (USA)	Robert Allman	RAL	exp	inexp
	Ashley Pacicco	APA	inexp	inexp
Institut de Recherche pour le Développement, UMR 212 EME IRD/Ifremer/UM2, Sete (France)	Fany Sardenne	FSA	exp	inexp
Hellenic Centre for Marine Research, Hiraklion, Crete (Greece)	George Tserpes	GTS	inexp	exp
Large Pelagics Group, St. Andrews Biological Station, St.Andrews (Canada)	Dheeraj Busawon	DBU	exp	inexp
Bluefin Tuna Resources Division, National Research Institute of Far Seas Fisheries, Fisheries Research Agency, Shimizu (Japan)	Taiki Ishihara	TIS	exp	inexp
Gulf Coast Research Laboratory, Ocean Spring, MA (USA)	Patricia Lastra Luque	PLL	exp	exp
School of Marine Sciences, The University of Maine/Gulf of Maine Research Institute, Portland, Maine (USA)	Elise Koob	EKO	exp	exp
CSIRO Marine and Atmospheric Research, Hobart, Tasmania (Australia)	Jessica Farley	JFA	exp	inexp

Ageing interpretation and precision

The CV and APE were estimated by CS and reader experience (Table 7.2). CV ranged between 17 and 22 with lower values for spines than for otoliths and for experienced in comparison with inexperienced readers. APE values range from 13 to 17 with the same trends.

Table 7.2 – Coefficient of variation (CV) and average per cent error (APE) by calcified structure for all readers and by reading experience (EXP= experienced, INEXP= inexperienced).

Calcified structure and light type	CV_ALL	CV_EXP	CV_INEXP	APE_ALL	APE_EXP	APE_INEXP
Otoliths Reflected Light (OR)	21.0	18.2	17.7	14.3	12.9	13.3
Otoliths Transmited Light (OT)	20.0	18.6	22.2	15.0	13.8	16.7
Spines Transmited Light (ST)	18.9	16.7	20.2	14.04	11.7	15.2

Analyzing CV trend by age and reader experience, Figure 7.1, it can be seen that the CV in otoliths was higher for the first five years and especially for non-experts, but after that remains constant and was similar for both types of experience. In spines better overall precision with respect to otolith was observed, but less precision at ages 1 and 2 and an increase in variability with age was observed for inexperienced readers. The decrease in the precision of the interpretation of otoliths for the first ages is probably related to the difficulty in interpreting the first five annuli. In spines, the occurrence of false first annulus (or cero annulus) may justify the greater variability of the first two annuli.

The influence of experience in the age interpretation and its relative accuracy is represented in Figure 7.2. Inexperienced reader age interpretations from otoliths under reflected light slightly overestimate age in relation to experienced readers ($p<0.01$), while otoliths viewed under transmitted light showed no tendency for the type of experience. For spines, inexperienced readers underestimated ages from 12 years upwards and increased the variability of their interpretations, although the relative bias was not significant ($p>0.05$). Therefore, it seems that the reading experience is a major factor in the age interpretation from otoliths viewed under reflected light and for large specimens using spines under transmitted light.

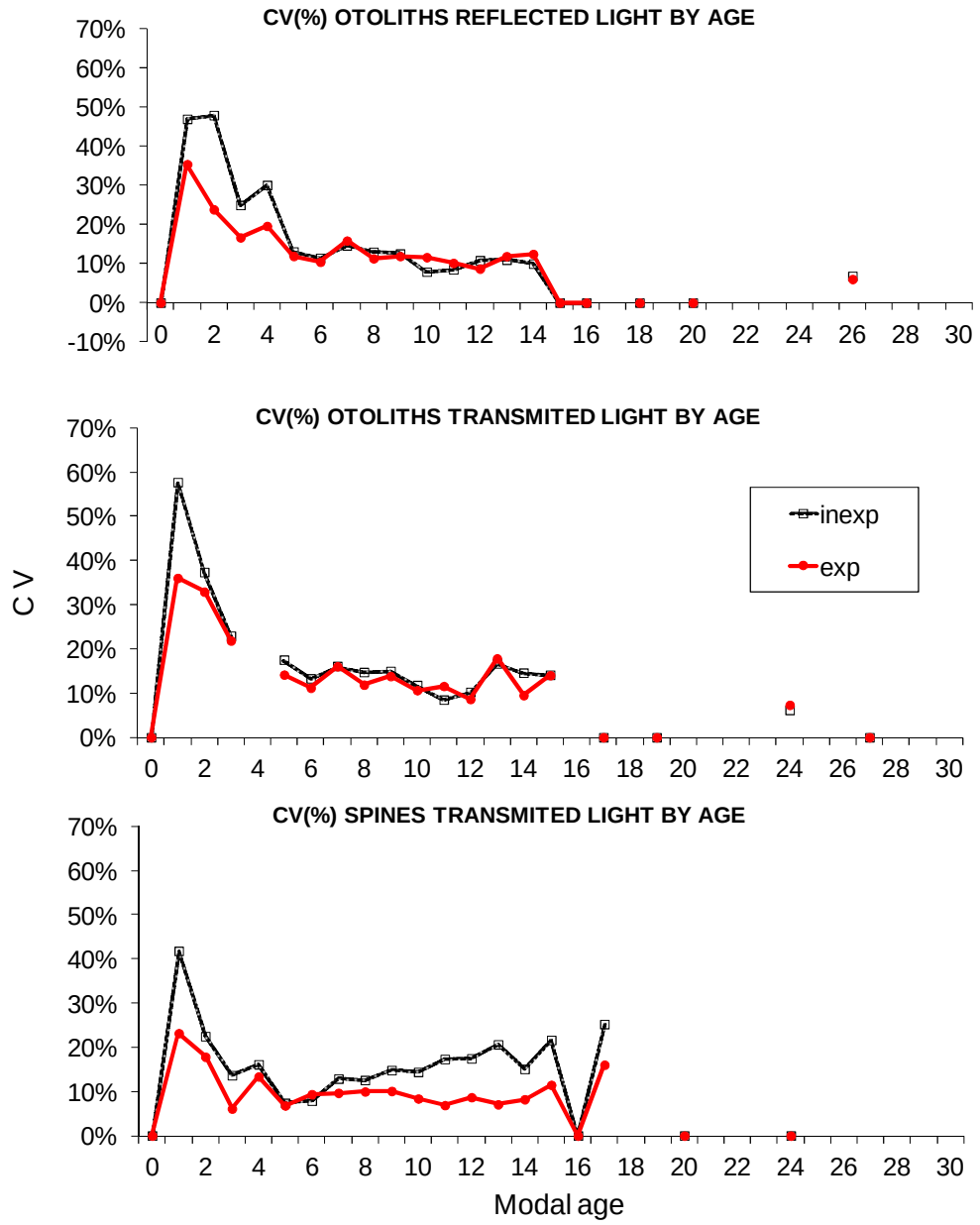

Figure 7.1- CV (%) trend by age and by calcified structure/type of light and reader experience (exp= experienced, inexp= inexperienced).

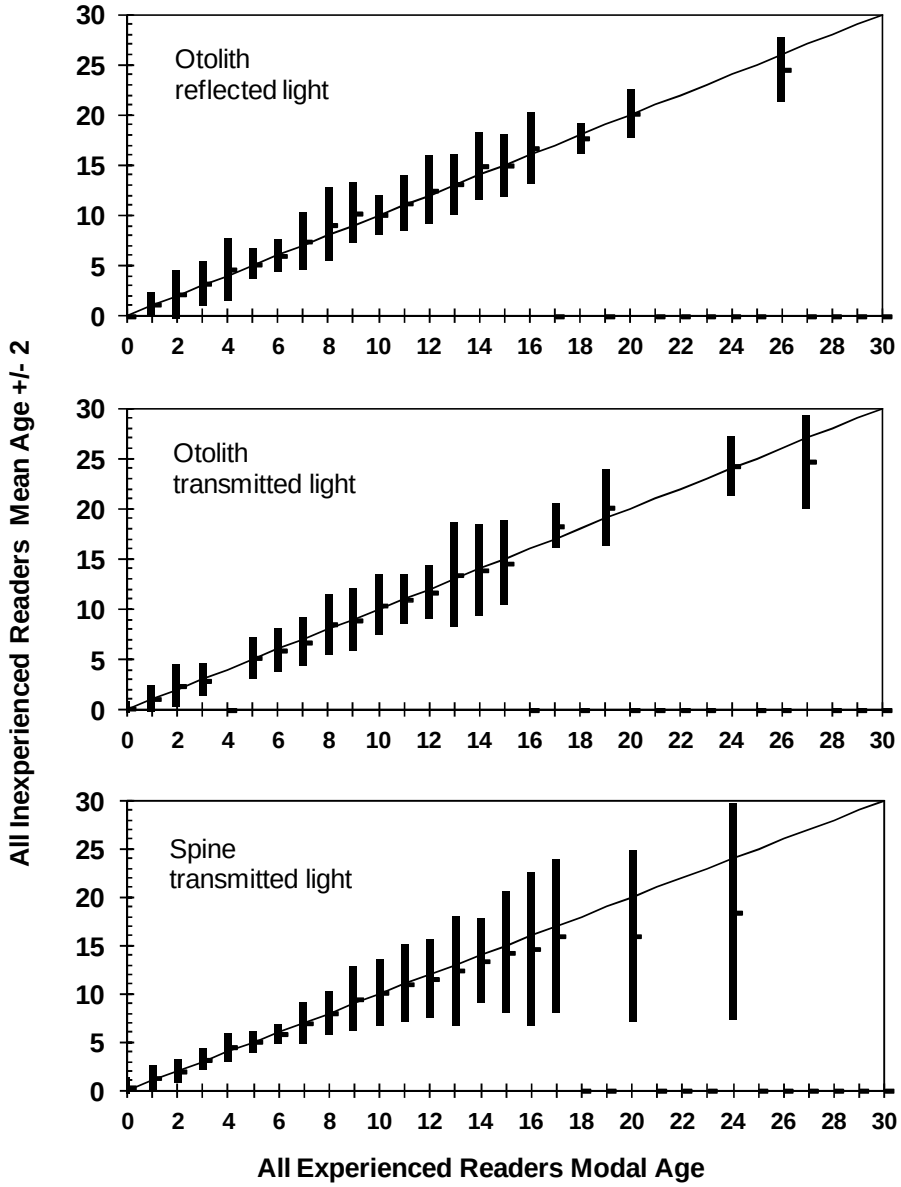

Figure 7.2 - Age bias plots representing the mean age recorded +/- 2stdev of all inexperienced readers combined plotted against the MODAL age from experienced readers by calcified structure and light type. Solid line is the 1:1 equilibrium line.

Quality of the calcified structure preparations.

The perception of the quality of the spine and otolith sections was generally good, despite sections not having been selected for their quality. Quality values by type of structure/ light were very similar, although skilled readers assigned slightly higher quality values (Table 7.3.). The Figure 7.3 shows that the quality of the otolith sections, using both types of light remained constant throughout the age range, although the first

three years were perceived with slightly lower quality. In spines quality got worse as age increased, which is possibly due to the greater difficulty in interpreting this CS in large specimens.

Table 7.3. – Mean sample quality by calcified structure/light and reading experience. EXP= experienced, INEXP= inexperienced, Readability Code: 1=Pattern present-no meaning, 2=Pattern present-unsure with age estimate, 3=Good pattern present-slightly unsure in some areas, 4=Good pattern-confident with age estimate.

Calcified structure and light type	SampleQuality_ALL	SampleQuality_EXP	SampleQuality_INEXP
Otoliths Reflected Light (OR)	2.87	2.93	2.76
Otoliths Transmited Light (OT)	2.84	2.86	2.79
Spines Transmited Light (ST)	2.94	2.99	2.88

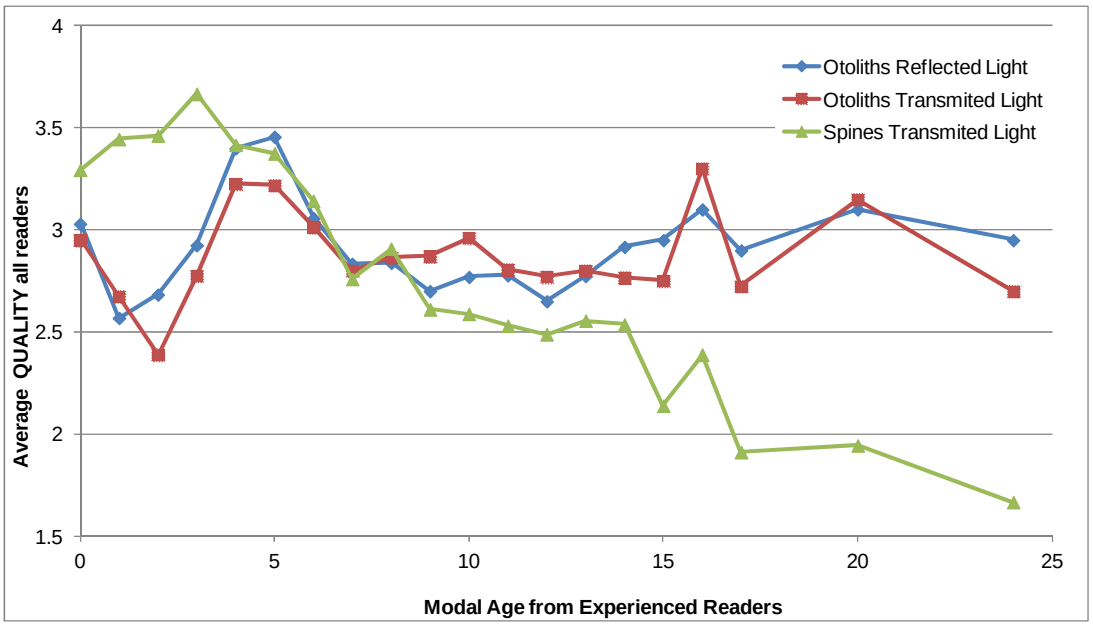

Figure 7.3 Average quality by CS/light type versus experienced reader modal age. Readability Code: 1=Pattern present-no meaning, 2=Pattern present-unsure with age estimate, 3=Good pattern present-slightly unsure in some areas, 4=Good pattern-confident with age estimate.

Edge type interpretation.

The agreement in the interpretation of CS sections edge, translucent or opaque, was analyzed by CS / light type using the percentage of agreement according to the most frequent assigned edge type. The values ranged from 72% for otoliths viewed under transmitted light and 77% for the spines seen under transmitted light. Monthly pattern in edge type was not appreciated in any of the CSs. The percentage of agreement among readers did not improve with increasing quality of the samples, except for spines which showed a slight greater agreement with increasing quality. For edge type assignment analysis by sample Figure 7.4 was prepared. Light did not appear to be a factor for otoliths as tile plots showed the same pattern under both light types. By contrast, the opposite pattern was found for spines.

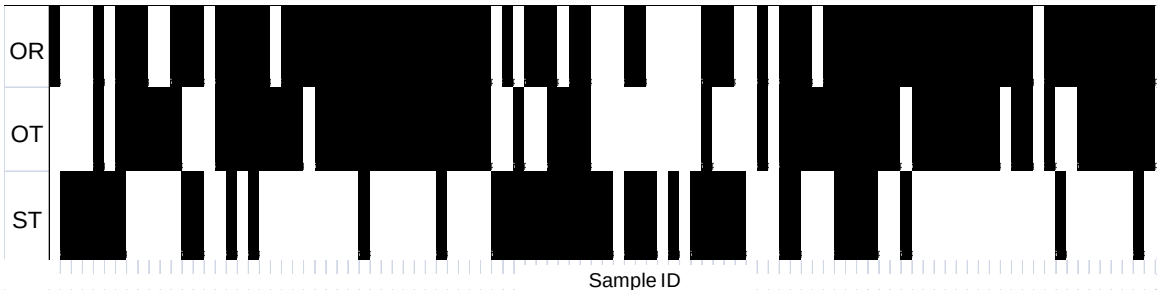

Figure 7.4 . - Tile plot of edge type assigned by CS/ light type for a given sample. OR= otoliths reflected light, OT= otoliths transmitted light, ST= spines transmitted light (black = Opaque, white = Translucent).

Ageing comparison between calcified structures and light type

Age interpretation among paired structures coming from the same specimen were compared (Figure 7.5). The comparison of age interpretation from otoliths using different types of light showed a good agreement, with no significant bias ($p>0.05$). Spine age interpretations showed no sign of bias with respect to otoliths viewed under transmitted light ($p>0.05$) but a slight under ageing when compared with reflected light otoliths ($p<0.05$), with these differences been found in specimens older than 14 years, for which the number of samples was very small.

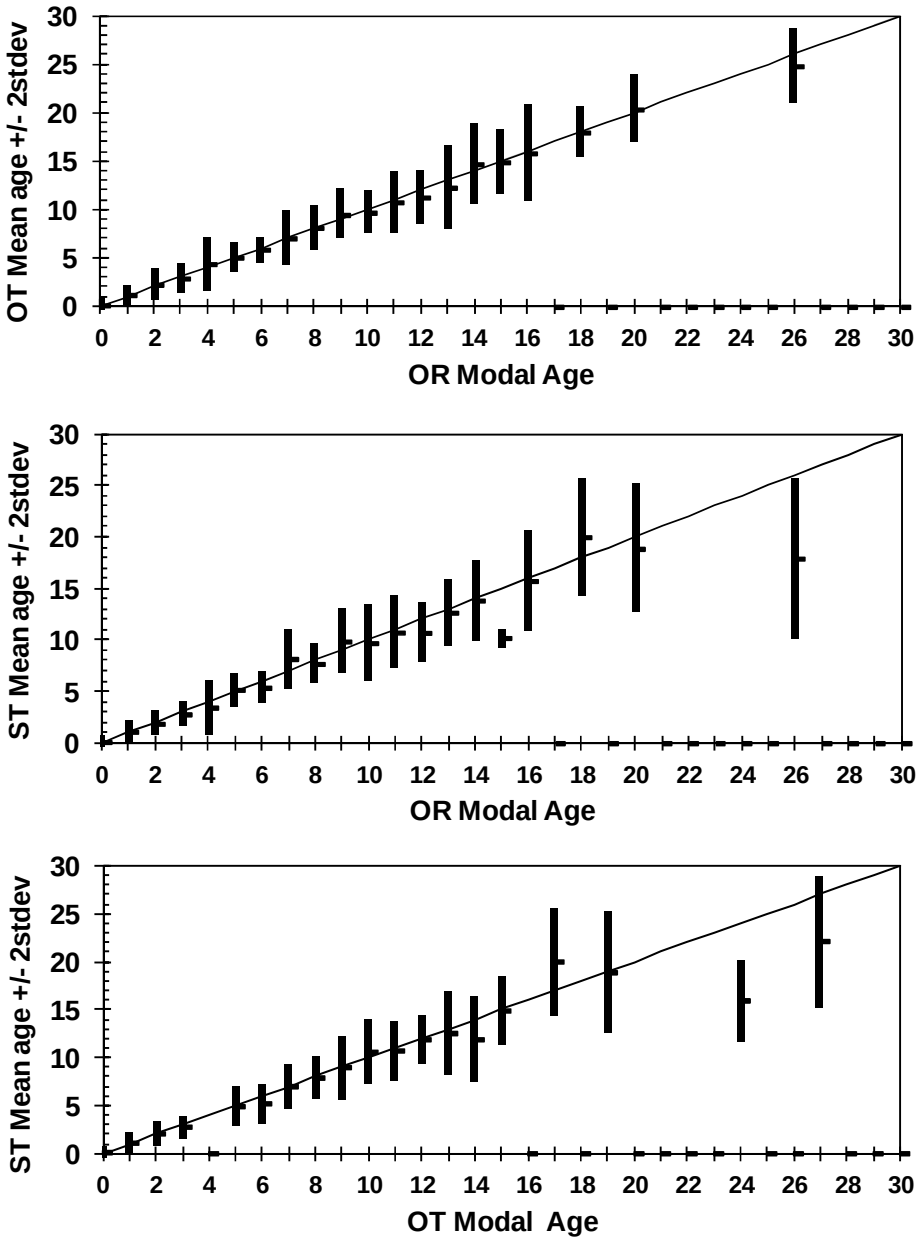

Figure 7.5 - Age bias plots representing the mean age recorded +/- 2stdev of experienced readers combined plotted against the MODAL age from experienced readers by calcified structure and light type. Solid line is the 1:1 equilibrium line. OR= otoliths reflected light, OT= otoliths transmitted light, ST= spines transmitted light

This is just a draft summary of the report of this section. The final report of the exchange will be agreed among the participants and shall be completed by September 15, 2014, for presenting the report as a SCRS paper to the BFT Species Group on the September 22.

References

- Busawon, D., Rodriguez-Marin, E., Lastra, P., and other authors. 2014. Evaluation of an Atlantic bluefin tuna Otolith Reference Collection. ICCAT, SCRS/2014/038
- Campana, S. E. 2001. Accuracy, precision and quality control in age determination, including a review of the use and abuse of age validation methods. J Fish Biol, 59(2):197-242.
- Campana, S.E.; Annand, M.C.; Mcmillan, J.I. 1995. Graphical and statistical methods for determining the consisteny of age determinations. Transactions of the American Fishery Society. 124:131-138
- ICCAT, 2013. Report of the 2013 Bluefin Tuna Meeting on Biological Parameters Review. pp. 11–12. Tenerife.
- Eltink, A.T.G.W. 2000.Age reading comparisons. (MS Excel workbook version 1.0 October 2000) Internet: http://efan.no.
- Kell, L. T. and Ortiz, M. 2011. A comparison of statistical age estimation and age slicing for Atlantic Bluefin tuna (Thunnus thynnus). Collect. Vol. Sci. Pap. ICCAT, 66(2), 948-955.
- Luque, P.L., Rodriguez-Marin, E., Ruiz, M., Quelle, P., Landa, J., Macias, D., Ortiz de Urbina, J.M. 2014. Direct ageing of Thunnus thynnus from the east Atlantic and western Mediterranean using dorsal fin spines. J Fish Biol 84, 1876-1903
- Neilson, J. and S. Campana. 2008. A validated description of age and growth of western Atlantic bluefin tuna (Thunnus thynnus). Can. J. Fish.Aquat. Sci. 65: 1523-1527.
- Rodriguez-Marin, E., Luque, P.L., Busawon, D., Campana, S., Golet, W., Koob, E., Neilson, J., Quelle, P., Ruiz, M. 2013. An attempt of validation of Atlantic bluefin tuna (Thunnus thynnus) ageing using dorsal fin spines. ICCAT, SCRS/2013/081